Journal Pre-proof

Structural architecture and the episodic evolution of the ediacaran Campo Alegre Basin (southern Brazil): Implications for the development of a synorogenic foreland rift and a post-collisional caldera volcano

Lucas Martins Lino, Francy Roxana Quiroz-Valle, Vinicius Louro, Miguel Ângelo Stipp Basei, Silvio Roberto Farias Vlach, Mathias Hueck, Patricio Rodrigo Montecinos Munõz, Sérgio Brandolise Citroni

PII: S0895-9811(20)30689-1

DOI: https://doi.org/10.1016/j.jsames.2020.103147

Reference: SAMES 103147

To appear in: *Journal of South American Earth Sciences*

Received Date: 15 July 2020

Revised Date: 13 October 2020

Accepted Date: 28 December 2020

Please cite this article as: Lino, L.M., Quiroz-Valle, F.R., Louro, V., Basei, Miguel.Â.Stipp., Vlach, S.R.F., Hueck, M., Munõz, P.R.M., Citroni, Sé.Brandolise., Structural architecture and the episodic evolution of the ediacaran Campo Alegre Basin (southern Brazil): Implications for the development of a synorogenic foreland rift and a post-collisional caldera volcano, *Journal of South American Earth Sciences* (2021), doi: https://doi.org/10.1016/j.jsames.2020.103147.

Structural architecture and the episodic evolution of the Ediacaran Campo Alegre Basin (southern Brazil): Implications for the development of a synorogenic foreland rift and a post-collisional caldera volcano

Lino[A*], Lucas Martins; Quiroz-Valle[A], Francy Roxana; Louro[B], Vinicius; Basei[B, C], Miguel Ângelo Stipp; Vlach[B], Silvio Roberto Farias; Hueck[B], Mathias; Munõz[B], Patricio Rodrigo Montecinos; Citroni[D], Sérgio Brandolise,

[A] - *Programa de Pós-Graduação em Mineralogia e Petrologia, Instituto de Geociências, Universidade de São Paulo – USP;*

[B] - *Instituto de Geociências, Universidade de São Paulo – USP, Rua do Lago, 562, CEP 05508-080, São Paulo, SP, Brasil;*

[C] - *Centro de Pesquisas Geocronológicas da Universidade de São Paulo (CPGeo-USP);*

[D] - *Instituto de Agronomia, Universidade Federal Rural do Rio de Janeiro – UFRRJ, Rodovia BR-465, Seropédica, RJ, Brasil;*

**Corresponding author present address: Universidade de São Paulo, Instituto de Geociências, e-mail address: lucas.martins.santos@usp.br (L.M.Lino)*

ABSTRACT

During the last decades, tectonic models provided new insight into the evolution of the Luis Alves, Curitiba, and Paranaguá terranes, which are all limited by thrust and transpressive shear zones, nowadays outcropping only as deep crustal horizons and presenting poorly known lateral displacements. An essential puzzle piece to understanding the juxtaposition processes and evolution of these blocks in the Neoproterozoic lies in the Campo Alegre Basin in Southern Brazil, a volcano-sedimentary sequence deposited during the middle to late Ediacaran. Based on new U-Pb geochronological, structural, and aero-geophysical data, at least two main stages of filling and subsidence have been identified in this region, namely the basin and the caldera stages. In the *Basin Stage*, the regional collisional tectonics triggered the far-field stress resulting in a local extension at ~605 ± 5 Ma through the reactivation of NNW-SSE inherited basement structures. The deposition of the sedimentary basin finishes with the *Initial Volcanic Activity*, corresponding to a bimodal mildly alkaline, predominantly mafic and effusive volcanism. After the transition to a post-collisional setting, probably at ca. 595 Ma, regional extension led to the *Caldera Stage* of the basin, which had its volcanic peak at ca. 583-580 Ma, contemporaneous with the intrusive A-type magmatism of the nearby Graciosa Province. The Main Volcanic Activity corresponds to a predominantly alkaline silica-saturated, effusive to explosive magmatic manifestation culminating with the formation of a caldera-volcano. The volcanic products from both the initial and the main volcanic activities were raised to the surface mainly through NNW-SSE and ENE-WSW oriented

conduits, respectively reactivated and neo-formed during the collisional process. The crustal-scaled discontinuities associated with the development of the sedimentary basin have further controlled the subsidence of the caldera structure, which might be the main mechanism of preservation for these ancient volcano-sedimentary sequences in the evolution of the Campo Alegre Basin.

Keywords: Aero-geophysics; Sedimentary Basin; Structural inheritance/reactivation; Volcanism; U-Pb geochronology.

1. Introduction

The formation of the Gondwana supercontinent triggered the Brasiliano/Pan-African orogenic cycle (*ca.* ~900 Ma to 530 Ma, hereafter referred to as Brasiliano orogeny), which is characterized by the approximation, collision, and variably marginal deformation of several crustal segments. Evidence of these tectonic processes are preserved in the São Francisco, Paranapanema, Rio de la Plata, Congo, and Kalahari cratons, and the Luis Alves, Paranaguá, and Curitiba terranes (Silva *et al.*, 2005; Basei *et al.*, 2008, 2018; Brito-Neves *et al.*, 2014). These blocks exhibit contrasting crustal thickness and rheological properties, and were juxtaposed along extensive fold- and thrust-belts, which developed by oblique and anachronous collisions between South American and African cratons (Silva *et al.*, 2005). In Brazil, the Mantiqueira Province is one of the largest and most significant Neoproterozoic orogenic systems that resulted from these events (Almeida *et al.*, 1981). In it, three complex orogenic belts, the so-called Araçuaí, Ribeira, and Dom Feliciano, are mostly constituted by synorogenic granitoids, fold-and-thrust belts, and marginal basins, deformed and metamorphosed during the Brasiliano orogeny (*e.g.*, Almeida *et al.*, 1981; Brito-Neves and Cordani, 1991; Brito-Neves *et al.*, 1999).

The late- orogenic and transitional stages of the Brasiliano cycle were marked by the opening and infilling of several small, fault-bounded volcano-sedimentary basins (*i.e.*, Camaquã, Castro, Camarinha, Itajaí, Eleutério, Pouso Alegre, so-called transitional basins) deposited indiscriminately onto different terranes and tectonic domains (Brito-Neves, 2002; Teixeira *et al.*, 2004; Almeida *et al.*, 2010). These stages in southern Brazil also comprehend the installation of several post-collisional A-type granitoids (Kaul and Cordani, 2000; Gualda and Vlach, 2007; Passareli *et al.*, 2018). In general, these transitional volcano-sedimentary basins are commonly interpreted as controlled by mechanic subsidence, generated by strike-slip tectonics (*e.g.,* Teixeira *et al.*, 2004; Barão *et al.*, 2017). However, their main mechanisms of installation and geodynamic settings remain controversial, which led Almeida *et al.* (2010, 2012) to interpret all of them as part of a 1,500 km-wide continental rift system.

In this sense, there is a lack of consensus concerning the tectonic settings of these volcano-sedimentary basins, mostly due to the lack of geochronological information. Additionally, the scarcity of studies connecting the volcanogenic occurrences with the epiclastic sedimentation complicates the understanding of basin evolution. Exceptional cases include the Camaquã Basin, which represents the larger and most studied volcano-sedimentary basin among these transitional basins in the Mantiqueira Province. In it, at least four volcano-sedimentary depositional cycles occurred between 630 and 510 Ma, associated with distinct late- to post-orogenic tectonic settings. These cycles registered the overlaying of a foreland, a strike-slip, and another two extensional rift basins within the same depositional locus (Paim *et al.*, 2000, 2014). Moreover, there are other distinctive, volcanic-dominated occurrences among these transitional basins, where the volume of volcanogenic rocks exceeds more than ~70% of the depositional sequences. They include (1) the Castro Basin, (2) the Campo Alegre Basin and the Corupá sub-Basin, (3) the Guaratubinha Basin, and (4) the Sierra de Aguirre Basin in Uruguay. These volcanic-dominated sequences comprehend relatively thin proximal epiclastic deposits overlaid by a thick well-preserved pile of volcanogenic rocks, still preserving structural features of their volcanic edifices (*e.g.,* Citroni *et al.*, 2001; Teixeira *et al*., 2004; Barão *et al*., 2017; Quiroz-Valle *et al*., 2020; Silva-Lara *et al.*, submited).

Among these volcanic-dominated sedimentary sequences, the Campo Alegre Basin and the Corupá sub-Basin probably occurred as a single basin (Citroni *et al.*, 2001) and together they preserve the most complete section of the epiclastic, sub-volcanic, and volcanic sequences. However, the origin, structural framework, and tectonic setting of this basin, as well as its association with the post-collisional A-type plutonic occurrences, still lack detailed analysis and geochronological constraints. Some authors consider the Campo Alegre, Corupá, and Guaratubinha basins as part of a NE-SW-striking rift in the post-collisional setting (Almeida *et al*., 2010; 2012), based on the available ages of the volcanic successions (*e.g.* 595 ± 16 Ma and 598 ± 29 Ma - Cordani *et al.* (1999) and Basei *et al.* (1998), respectively), and the ages of the post-collisional granitoids. Alternatively, other authors consider this basin as an NNW-SSE-striking rift as part of the collisional tectonics, based on the sedimentary infilling processes and newly obtained provenance ages of 606 ± 4 Ma (Citroni *et al.*, 2001; Quiroz-Valle *et al.*, 2019).

In this sense, the present research aims to establish the tectonic setting of the Campo Alegre-Corupá volcano-sedimentary sequence and achieving a better age control for the volcanic activity. Based on geological, geophysical, and structural data, we discuss the major role of the collisional tectonics and inherited basement structures in the initial subsidence and filling processes of this basin, and the contribution of the volcanic activity in the form of a caldera volcano in the preservation of the sequences. Moreover, we discuss and constrain, with U-Pb zircon geochronological data, the initial and the main volcanic episodes in the Campo Alegre volcano-sedimentary basin. This information allows us to reevaluate the tectonic settings, in which the volcano-sedimentary sequences were generated, comparing these occurrences with other similar settings worldwide.

2. Geological Settings

The Luis Alves and Curitiba Terranes (**Fig.1**), which separate the exposed areas of the Ribeira and Dom Feliciano belts, both represent pre-existent continental fragments of unknown origin within the continental-scaled Brasiliano orogeny (Basei *et al.*, 1992; Brito-Neves *et al.*, 1999; Basei *et al.*, 2009; Passareli *et al.*, 2018). The Piên-Mandirituba calc-alkaline batholith and the Mafic-Ultramafic Piên Suite separate these terranes along with the Piên Shear Zone, and they are both interpreted as remnants of a magmatic arc and an incomplete ophiolite sequence, respectively (Harara, 2001; Harara *et al.*, 2004). The

LAT constitutes the oldest crustal segment in southern Brazil, occurring in between extensive supracrustal belts that affected mostly its boundaries during the Neoproterozoic (Basei *et al.*, 2000, 2008). The agglutination of crustal segments during the Brasiliano orogeny resulted in an intense marginal and superficial brittle deformation of the LAT, producing new structures and reactivating older zones of weakness (Basei *et al.*, 1992; Harara, 2001). These structures were presumably responsible for the origin and evolution of some of those transitional volcano-sedimentary basins (*e.g*. Campo Alegre-Corupá and Guaratubinha). Additionally, several A-type granites and syenites were formed during the orogenic late-stages in this region, in which these reactivated structures probably controlled the magma ascension and the emplacement of these granitoid plutons (Kaul and Cordani, 2000; Basei *et al*., 2009; Vlach *et al*., 2011).

The LAT comprises essentially two units; the first one comprehends the Archean to Paleoproterozoic migmatitic granitic-gneissic rocks from the Santa Catarina Granulitic Complex (SCGC - Hartmann *et al.*, 1979; Basei *et al.*, 1998), while the Neoproterozoic covers, gathered into three main volcano-sedimentary basins and other smaller widespread occurrences, represent the second one (Passareli *et al.*, 2018). Despite its relatively small size compared to other cratonic segments, the nucleus of the LAT remained cold and stable during the Brasiliano orogeny, at least since the latest Paleoproterozoic regional cooling, between ~1,700 – 1,800 Ma (*e.g.*, Basei *et al*., 2009; Passareli *et al*., 2018; Heller *et al.*, this issue). The SCGC comprehends primarily Archean to Paleoproterozoic migmatitic gneisses with TTG geochemical affinity, coupled to minor mafic layers interbedded with metasedimentary units. Alternating quartz-feldspathic and amphibole/pyroxene-rich mafic layers characterize this migmatites and orthogneisses (Hartmann *et al.*, 1979; Basei *et al.*, 1998; Basei *et al.*, 2009; Heller *et al.*, this issue). The presence of orthopyroxene suggests metamorphism at high-grades, which occurred under 5 – 7 kb with a thermal peak at ~800°C (Girardi and Ulbrich, 1978; Hartmann *et al.*, 1979). In the north domain of the LAT, near the Campo Alegre Basin, high-grade gneisses yielded U-Pb ages of 2,200 ± 4 Ma and 2,230 Ma. Similar ages were obtained in charnockitic-enderbitic rocks, 2,204 ± 30 Ma and 2,338 ± 37 Ma (Basei *et al.*, 2009) and in tonalitic gneisses associated with amphibolite, 2,183 ± 17 Ma and 2,352 ± 17. Ma (Heller *et al.*, this issue). Both age intervals are attributed to high-grade metamorphic events affecting Archean magmatic protoliths, and characterize the most significant tectonic processes registered by zircon U-Pb geochronology in the SCGC (Basei *et al*., 2009; Passareli *et al*., 2018). Retrograde metamorphism at ca. 2.0 Ga re-equilibrated the association in amphibolite-facies conditions, as constrained by the U-Pb dating of titanite (Heller *et al.,* this issue).

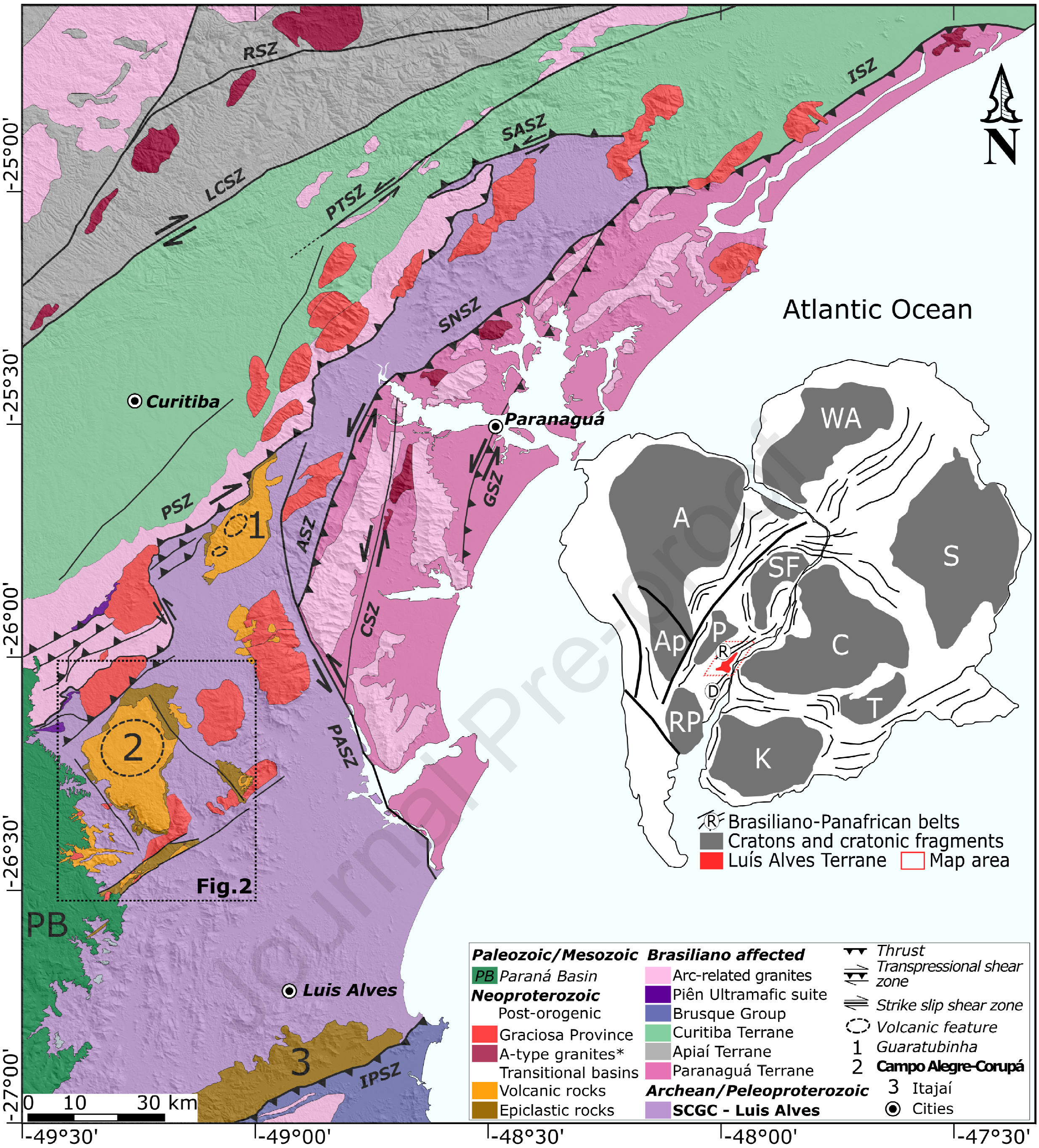

Figure 1: Simplified regional geotectonic map of southern Brazil, highlighting Neoproterozoic units and structures. (Modified after Harara, 2001; Gualda and Vlach, 2007; Basei et al., 2009; Patias et al., 2019). Main Map Legend: RSZ – Ribeira Shear Zone; LCSZ – Landinha-Cubatão Shear Zone; PTSZ – Putunã Shear Zone; SASZ – Serra do Azeite Shear Zone; ISZ – Icapara Shear Zone; SNSZ – Serra Negra Shear Zone; PSZ – Piên Shear Zone; ASZ – Alexandra Shear Zone; GSZ – Guaratuba Shear Zone; CSZ – Cubatãozinho Shear Zone; PASZ – Palmital Shear Zone; IPSZ – Itajaí-Perimbó Shear Zone. Cratons Inset: A – Amazonia; Ap – Rio Apa; C – Congo; K – Kalahari; Luis Alves (red); P – Paranapanema; RP – Rio de la Plata; S – Sahara; SF – São Francisco; T – Tanzania; WA – West-Africa. Orogenic Belts in the inset R – Ribeira and D – Dom Feliciano. (*) Other Neoproterozoic post-collisional and A-type granitoids that are not included in the Graciosa Province. SCGC – Santa Catarina Granulitic Complex, the basement of the Luis Alves Terrane.

Intrusive stocks and plutons, mainly exhibiting oval-shaped to irregular geometries, were a consequence of the post-collisional stages of the Brasiliano orogeny in the LAT, at approximately 580-583 ± 3 Ma (Vlach *et al.*, 2011; Vilalva *et al.*, 2019). These intrusions are predominantly composed of A-type granites and syenites, with subordinate gabbros, K-rich diorites, and monzodiorites, associated with volcanic and sub-volcanic occurrences, constituting the Graciosa Province (Gualda and Vlach, 2007; Vilalva & Vlach, 2014). As a whole, these plutons are aligned with the present-day Brazilian coastline. The most voluminous occurrences, estimated based on their exposed surfaces, are concentrated at the southern portion of the province, close to the central region of the LAT, and circuiting the Campo Alegre-Corupá Basin. They are mainly intruding in the LAT basement, while further being intrusive in the Piên-Mandirituba batholith, and in the Curitiba and Paranaguá Terranes at shallow crustal levels (~2 to ~5 km depth; Gualda and Vlach, 2007; Vilalva and Vlach, 2014). The coexistence of two distinct petrographic associations, an alkaline and an aluminous one, is the main characteristic of these A-type granites and syenites. The alkaline association comprises metaluminous to peralkaline alkali feldspar to hypersolvus granites, whereas the aluminous association includes metaluminous to peraluminous subsolvus syeno- and monzogranites (*cf.* Gualda and Vlach, 2007).

2.1. Neoproterozoic volcano-sedimentary covers and the Campo Alegre-Corupá Basin

The Campo Alegre-Corupá Basin (CACB) and the Guaratubinha Basin are both fault-bounded volcano-sedimentary basins, located close to the northern boundary of the LAT with ~550 km^2 and ~200 km^2 in area, respectively (**Fig.1**). Both are predominantly constituted by volcanogenic sequences, covering up to 75 – 90% of the basins area, deposited between ~605 – 580 Ma (Ebert, 1971; Citroni *et al.*, 2001; Basei *et al.*, 2009; Barão *et al.*, 2017; Quiroz-Valle *et al.*, 2019; this study). The Itajaí Basin, on the other hand, is also a volcano-sedimentary basin of the southern margin of the LAT basement, thought to have been formed as a foreland depocenter, originated during the collisional stage of the Dom Feliciano Belt, at ~600 – 560 Ma (*e.g.*, Basei *et al.*, 2011; Hueck *et al.*, 2018). The development and infilling processes of the CACB (**Fig.2**), as well as the Guaratubinha Basin, are considered to be related with the regional deformation induced by the collisional, or alternatively by the post-collisional, events during the Brasiliano orogeny (Basei *et al.*, 1998; Citroni *et al.*, 2001; Almeida *et al.*, 2010; Barão *et al.*, 2017, Quiroz-Valle *et al.*, 2019). The divergences in the interpreted tectonic settings are mostly due to the lack of well-constrained depositional ages for the volcanic sequences.

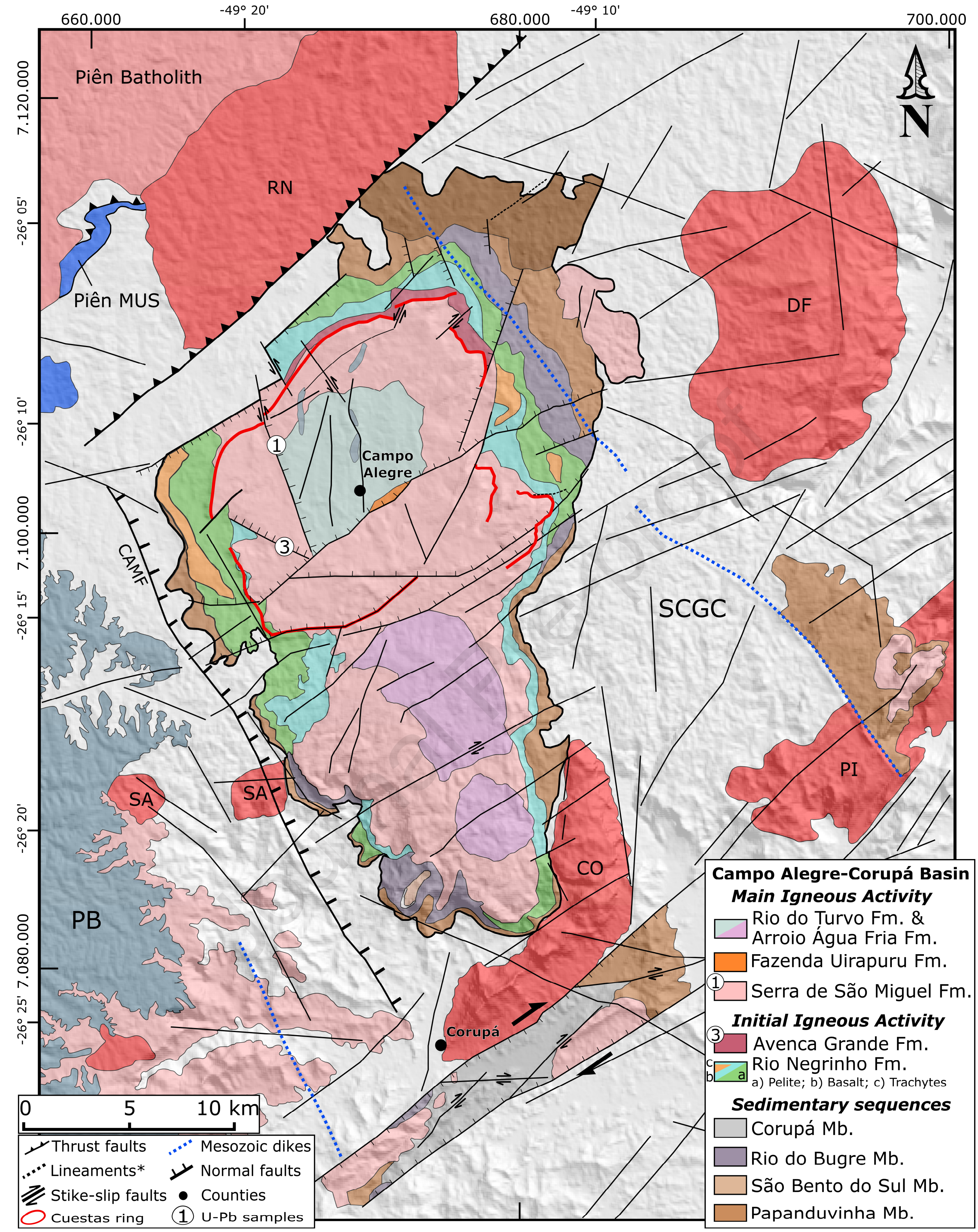

Figure 2: *Geological map of the Campo Alegre-Corupá Basin illustrating the regional distribution of the main geological units and surrounding plutonic occurrences (modified after Citroni et al., 2001). (*) Geophysical and geomorphological lineaments; CAMF – Campo Alegre Master Fault. The circled numbers 1 and 3 represent the location of samples PPW-01 and PPW-03, respectively, close to major fault zones in the northern region of the Campo Alegre Basin. The relative position of the dated rocks is given in the legend. SCGC – Rocks from the Santa Catarina Granulitic Complex; Surrounding granitoids: CO – Corupá; PI – Piraí; RN – Rio Negro; SA – Serra Alta; DF – Dona Francisca. PB – volcano-sedimentary sequences from the Paraná Basin. Piên MUS – Piên Mafic-Ultramafic Suite.*

All depositional sequences observed in the CACB were also identified in the Guaratubinha basin (Daitx, 1979; Daitx and Carvalho, 1981), including a lower sedimentary sequence covered by a thick bi-modal, volcanic sequence. These similarities might suggest that these basins are remnants of previously connected depocenters, further supported by similar U-Pb zircon ages obtained from rhyolites in the volcanic cover (Basei *et al.*, 1998). In the CACB, Citroni *et al.* (2001) has defined two main stages of infilling, so-called the Pre-volcanic and the Volcanic stages, represented by the sedimentary and volcanogenic sequences, respectively. These authors consider the evolution of the CACB as a continuum process, evolving from a sedimentary basin to a caldera volcano uninterruptedly through time. However, due to intrinsic depositional characteristics of the volcanogenic deposits, further detailed in this section, and compositional features as pointed out by Lino *et al.* (2020), we divided the volcanic stage into other two main periods, hereafter referred to as the *Initial Volcanic Activity* and the *Main Volcanic Activity*.

The *Pre-volcanic stage* of the CACB represents its initial deposition, characterized by a dominantly ruditic, proximal, and immature sedimentary strata, corresponding to the Bateias Formation (Citroni *et al.*, 2001). Outcrops of this unit are restricted to the basin boundaries (**Fig.2**). The sedimentary sequence overlies the high-grade metamorphic rocks from the LAT, (*e.g.*, **Fig.3a**), which represents one of the main source-areas for these sedimentary rocks (*e.g.*, **Fig.3b**), coupled with the granitic and possibly volcanic rocks from the Piên Magmatic Arc (*cf.*, Citroni *et al.*, 2001; Quiroz-Valle *et al.*, 2019). Three members, corresponding to different depositional facies, constitute the Bateias Formation: (1) the Papanduvinha, (2) São Bento do Sul, and (3) Rio do Bugre members. The Papanduvinha Member corresponds to massive, poorly sorted polymictic breccias and fanglomerates, occurring at the basin northern margin. The São Bento do Sul Member corresponds to a conglomeratic facies deposited by braided rivers, with stratification and imbrication of pebbles. Finally, the Rio do Bugre Member corresponds to a facies of sandy and pelitic sediments, deposited in fluvial and subaqueous environments. Within these sedimentary sequences, Valiat (1974) describes the episodic occurrence of thin layers (< 20 cm) of ash fall tuffs founded in exploratory body holes, more frequently present at the uppermost deposits. Compositional, textural, and provenance analysis indicates a common source for these sedimentary units, deposited according to a general NW-to-SE trend of transportation and reworking (Citroni *et al.*, 2001; Quiroz-Valle *et al.*, 2019).

The *Initial Volcanic Activity* is an effusive-dominated occurrence, marked mainly by basaltic to andesitic lava flows (**Fig.3c**), commonly interbedded with fine-grained sandy and pelitic sedimentary rocks, defining the Rio Negrinho Formation (Citroni *et al.*, 2001). These sequences are also associated with acid effusive occurrences, essentially of trachytic composition, and coupled to subordinated rhyolitic lavas. Several structural and textural evidence in the lava flows and laminated pelites, such as hyaloclastite fragmentation, fragments of lava-flows associated with fine-grained sediments, and lavas in pillows, attest to the continuity of the subaqueous conditions from the previous pre-volcanic stage (Citroni *et al*., 2001). These earlier depositional stages occurred within a lake or epicontinental sea, during the initial effusive activity (*cf.*, Citroni, 1998; Citroni *et al.*, 2001). Covering these previous deposits, a sequence from a *surge-like* pyroclastic deposit defines the Avenca Grande Formation. Within this pyroclastic sequence, it is possible to observe eroded and partially weathered fragments of basaltic and andesitic rocks, as well as evidence of pyroclastic-flows within waterbodies, such as horizons with braided stratification intercalated in laminated siltite (Citroni *et al.*, 2001).

The *Main Volcanic Activity* is an explosive-dominated occurrence, characterized by extensive and voluminous pyroclastic and minor effusive silicic sequences (Citroni *et al.*, 2001). It is composed mainly of massive- to welded-ignimbrites, coupled to minor rheomorphic-ignimbrites and lava flows presenting rhyolitic and trachytic compositions (**Figs.3d-f**; Citroni *et al.*, 2001; Quiroz-Valle *et al.*, 2020). Both explosive and effusive occurrences are gathered into the Serra de São Miguel Formation, covering almost 75% of the basin area, corresponding to the thickest and most characteristic volcanic unit in the CACB. The deposition of these sequences occurred in predominantly subaerial conditions. The uppermost sequences include high-grade ignimbrites covered by acid lava flows, forming an almost circular ring of cuestas at the CACB north zone (**Fig.2**). These sequences show depositional structures with low dipping angles towards the central region, probably corresponding to a preserved caldera structure (Citroni *et al*., 2001; Quiroz-Valle *et al.*, 2020). During the caldera stage, volcanogenic fine-grained sediments and silicic lava flows characterize the intra- (Rio Turvo Formation) and extra-caldera (Arroio Água Fria Formation) deposition, respectively. The intra-caldera lake deposits occupy an area of nearly 45 km^2, reaching up to 150 m of thickness (Valiat, 1974; Citroni *et al.*, 2001). Lake sedimentation alternates with some periods of volcanoclastic activity, registered as ash fall tuff layers interbedded with pelitic rocks. There is further evidence of a significant hydrothermal period in this area, especially during the caldera quiescence (Citroni *et al.*, 2001), which is registered in the occurrence of Kaolin deposits (Biondi *et al.*, 2001a, b; Biondi *et al.*, 2002; Oliveira *et al.*, 2007).

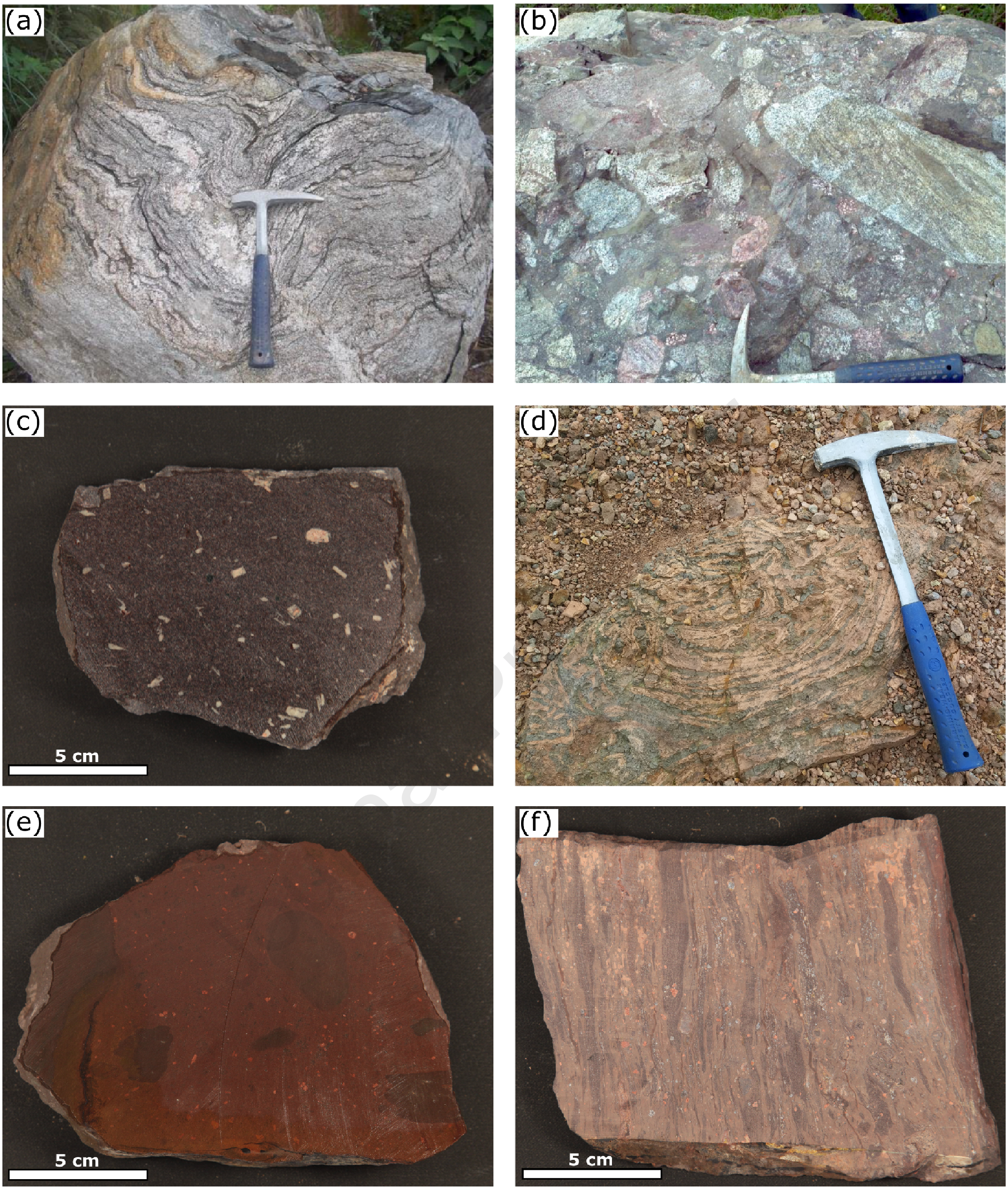

Figure 3: *(a) Field aspects of the metamorphic rocks from the Santa Catarina Granulitic Complex. The photographs illustrate typically folded migmatite of the western limit of the CACB. (b) Field aspects of the conglomeratic rocks from the Papanduvinha member, containing clasts from metamorphic, plutonic, and volcanic origin (cf., Quiroz-Valle et al., 2019). (c) Hand sample of andesite (andesitic basalt) from the Rio Negrinho Formation. Note the porphyritic texture given by plagioclase phenocrysts. (d) Filed aspects of flow-banded rhyolites from the Serra de São Miguel Formation. Primary flow-structures and spherulites are well preserved. (e) Hand sample of a trachytic autoclastic lava-flow containing K-feldspar phenocrysts. (f) Hand sample of a high-grade welded crystal-rich ignimbrite containing quartz and K-feldspar. The primary volcanic eutaxitic texture is well preserved.*

3. Methods and Analytical Procedures

The database of this contribution includes structural field data, available aerial geophysics data (CPRM, 2011) and digital elevation models, and newly obtained zircon U-Pb geochronology results. Geophysical data processing and treatment procedures were performed in the Geosoft's Oasis Montaj software, following Louro *et al.* (2014, 2017), and Lino *et al*. (2018). Regional investigation using magnetic field data was supported by the use of enhancement techniques as the Tilt Derivative (Miller and Singh, 1994). Complementing the magnetic evaluation, the Euler Deconvolution (Reid *et al*., 1990) was used to estimate the relative depth of lineaments, specifically in the region of the CACB, following Reid *et al.* (2014), and Reid and Thurston (2014). Based on 2D images combining geomorphological and geophysical lineaments in the region of the CACB, quantitative analysis of these structures was conducted using the FracPaQ toolbox (*e.g.*, Healy *et al*., 2017). For additional details on the analytical methods for the geophysical and structural characterization see Supplementary Material 1.

Two representative samples were collected within the major lower- and uppermost pyroclastic units defined by Citroni *et al.* (2001) for U-Pb geochronology (**Fig.2**). Zircon dating by Laser Ablation Multi-Collector Inductively Coupled Plasma Mass Spectrometry (LA-MC-ICP-MS) analysis was conducted in the Geochronology Research Center of the Universidade de São Paulo (IGc-USP), on an inductively coupled plasma (ICP) multi-collector (MC) Neptune (Thermo) spectrometer (MS), coupled to a 193 nm Excimer Laser (Photon Machines). Data were reduced using SQUID 1.02 (Ludwig, 2001) and plotted using the Excel add-in ISOPLOT 4.11 (Ludwig, 2003) over Tera-Wasserburg diagrams. Additional details on the main methods and analytical procedures are provided in the Supplementary Material 1. Petrographic characterization of the dated samples, the detailed analysis of the morphological aspects of the dated zircon crystals, and statistical procedures applied for the geochronological data are provided in the Supplementary Material 2.

4. Geophysical framework

4.1. Luis Alves Terrane

The exposed area of the LAT basement extends for approximately 255 km in the northeast-southwest direction, and *ca.* 85 km in the east-west direction (**Fig.4a**). The anomalous magnetic field in the area has an amplitude of 3,980 nT (-1,753 to 2,227 nT), with the highest values marked by the NW-SE signatures caused by the Cretaceous mafic dike swarms associated with the Ponta Grossa Arc (*e.g.*, Riccomini *et al.*, 2005). These magnetic lineaments display a clear short-wavelength behavior, although some of them might display longer wavelengths (**Fig.4b**). The anomalous magnetic field to the northeast and the southeast of the dike-swarm present elongated anomalies, following the preferential NE-SW structural configuration of the Precambrian basement. The southern area of the Terrane has an oval magnetic structure 60 km long wide, in an area characterized by the high-grade Pomerode orthogneisses, occurring between the CACB and Itajaí basin (Basei *et al.*, 2009). The Upward Continued fields followed by a Tilt Derivative filtering highlight longer-wavelength magnetized sources of the region

(**Fig.4c**). We defined the altitudes of the Upward Continued fields based on the radial spectrum behavior of the anomalous filed. An RGB composition of multiple altitudes fields (0, 1,000, and 2,000 m) permitted to highlight the continuity of lineaments into the crust and to divide them into different sets, based on their general orientation and wavelengths (**Fig.4d**).

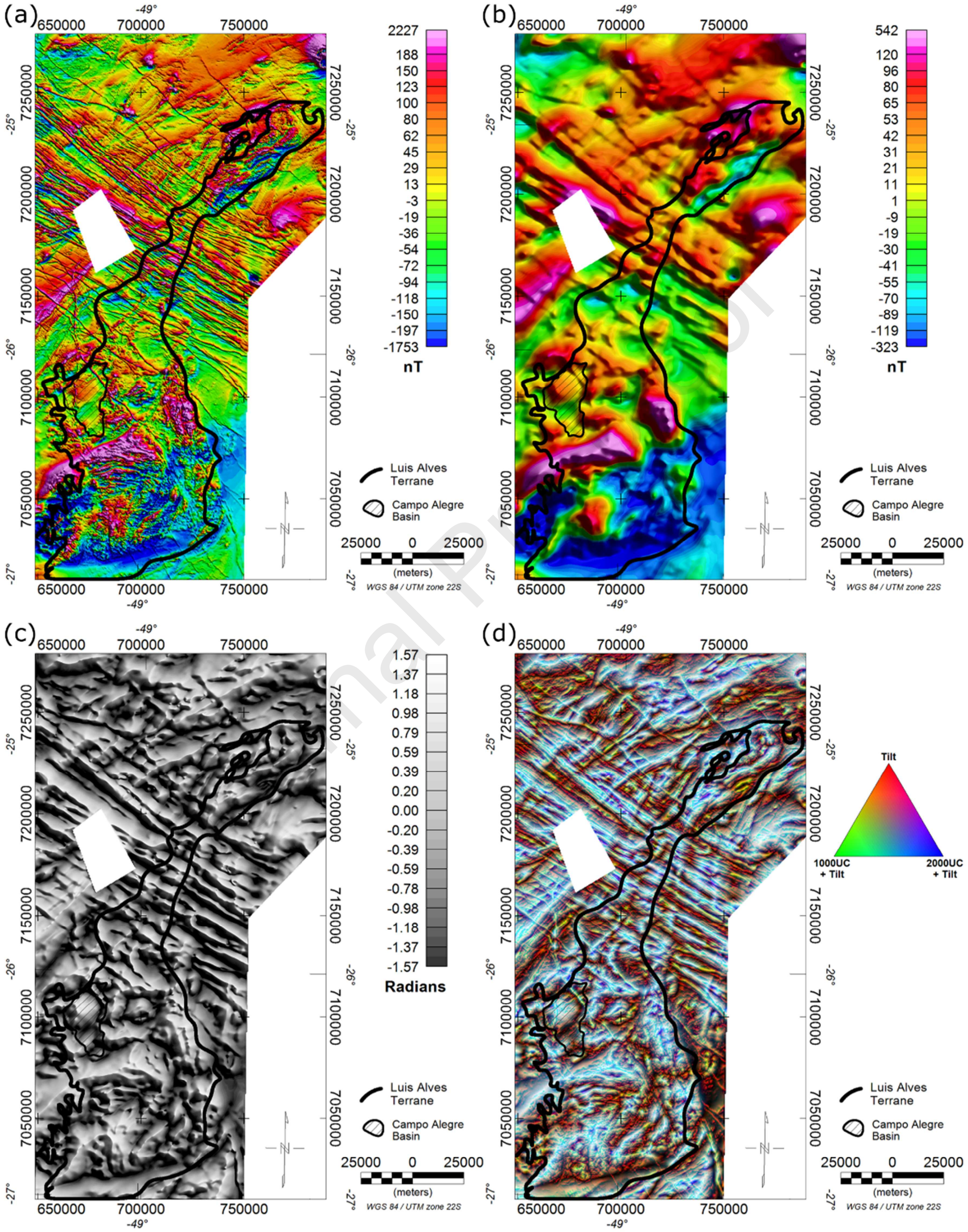

Figure 4: *Luis Alves Terrane area: (a) anomalous magnetic field. (b) 2000 m upward continued anomalous magnetic field. (c) 2000 m upward continued anomalous magnetic field followed by a Tilt Derivative filtering. (d) Ternary image composed by the Tilt Derivative (Tilt - red), the 1000 m upward continued field followed by the Tilt Derivative (1000UC + Tilt – green), and the 2000 m upward continued magnetic field followed by the Tilt Derivative (2000UC + Tilt – blue).*

The overall behavior of the main crustal-scale lineaments highlighted in the geophysical regional maps is summarized in **Fig.5a** grouped according to their average orientation. These lineaments define three structural domains, overprinted by the Cretaceous dike swarm, constrained to the northern sector. The first regional trend, oriented at N60°Az predominates north of the LAT and into its northern portion and can be associated with the major regional shear zones, such as the Alexandra, Lancinha-Cubatão, Mandirituba-Piraquara, and Serra Negra (*cf.* **Fig.1**). The remaining two sets of lineaments predominate in the central and southern regions of the LAT. The southernmost set limits the 60 km oval structure also recognized in **Fig.4** and delimits the Itajaí Basin and the border of this basin along the Itajaí-Perimbó Shear Zone further to the south. The central set of lineaments appears in the region of the CACB and presents three main orientations. The first is subparallel (N145°Az) to the Palmital Shear Zone, which defines the southeastern border of the Terrane; the second set follows the general orientation of the Piên Shear Zone at the north (N55°Az); and the third set is defined by a single, approximately north-south-oriented lineament (N5°Az).

Based on radiometric data, the LAT can be divided into three sectors that roughly coincide with the defined structural domains (*cf.* **Fig.5b**). The northernmost Sector I, in which the terrane narrows and aligns with the overall northeast-southwest trend, displays lower counts of K, eTh, and eU, and it is equivalent to the area most affected by the Ponta Grossa dike-swarm. From north to south, a discrete predominance of K is replaced by an increasing presence of eTh until it reaches Sector II. The central Sector II shows the predominance of eTh along most of its extent, including in the area of the CACB. Three areas at the center and west of the Sector II presents considerably high counts of K and correspond to granitic bodies of the Graciosa Province. In the eastern area of this sector, very low counts of the three elements are mostly seen in the Quaternary, Paleogene, and Neogene coastal sediments. The southern Sector III coincides with the oval-shaped feature, representative of the orthogneisses Pomerode, seen in the magnetic field data and sub-products. This sector presents high counts of K and eTh, with the predominance of the latter in its eastern and western limits. In the north and south-central areas, a high K signature appear quite similar to those related to the Graciosa Province found within Sector II. A low counts area, with a slight dominance of eU, can be found in the central-eastern area.

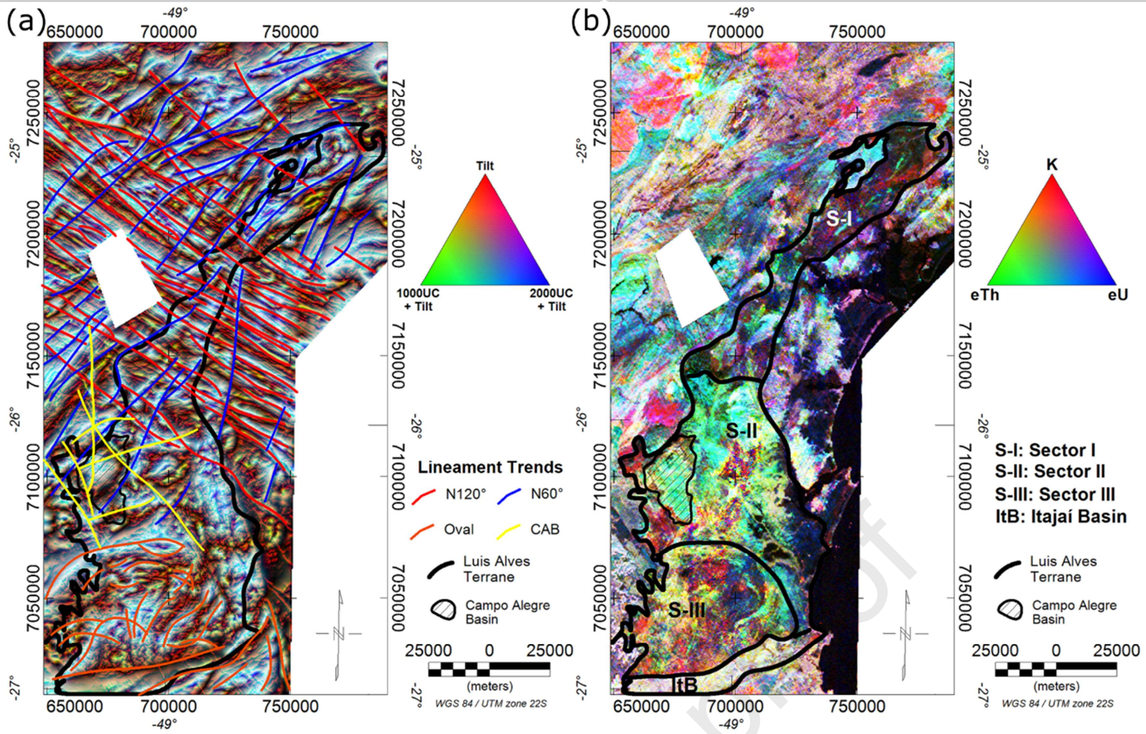

Figure 5: *(a) Composition of all sets of magnetic lineaments in the LAT area and surrounding terranes. (b) Radiometric ternary image of the LAT depicting the sectors of different radiometric response.*

4.2. Campo Alegre Basin

The anomalous magnetic field in the region of the CACB has an amplitude of 1,656 nT (-789 to 857 nT), which is much less expanded when compared with the regional data (**Fig.6a**). The CACB itself displays an almost constant magnetic field, without significant anomalous features within its mapped limits. The anomalous magnetic field of the region evidences three major lineaments, oriented at the N-S, NE-SW, and NNW-SSE directions, the latter delimiting the western border of the basin, coincident with the *Campo Alegre Master Fault* (*cf.*, **Fig.2**, Citroni *et al.*, 2001). The same Tilt Derivative routine exposed in **Section 4.1** was performed on the anomalous magnetic field of the CACB (**Fig.6b**) and after upward continuing the field to 500 m and 1000 m (**Fig.6c-d**). The last two grids allow evaluating longer wavelengths, representing shallow structures going into lower levels of the crust or deeper structures. Repeated composition of the Tilt Derivative with Upward Continued fields classified the lineaments according to their wavelength (**Table 1**) and orientation. In comparison with the regional structures, the NNW-SSE and NE-SE lineaments become more apparent in the area, showing coherent short-wavelength lineaments with the local trend of approximately N55°Az, as shown by the Piên Shear Zone. These lineaments are mostly restricted to higher grounds, whereas medium wavelengths are rare and do not present a preferential direction.

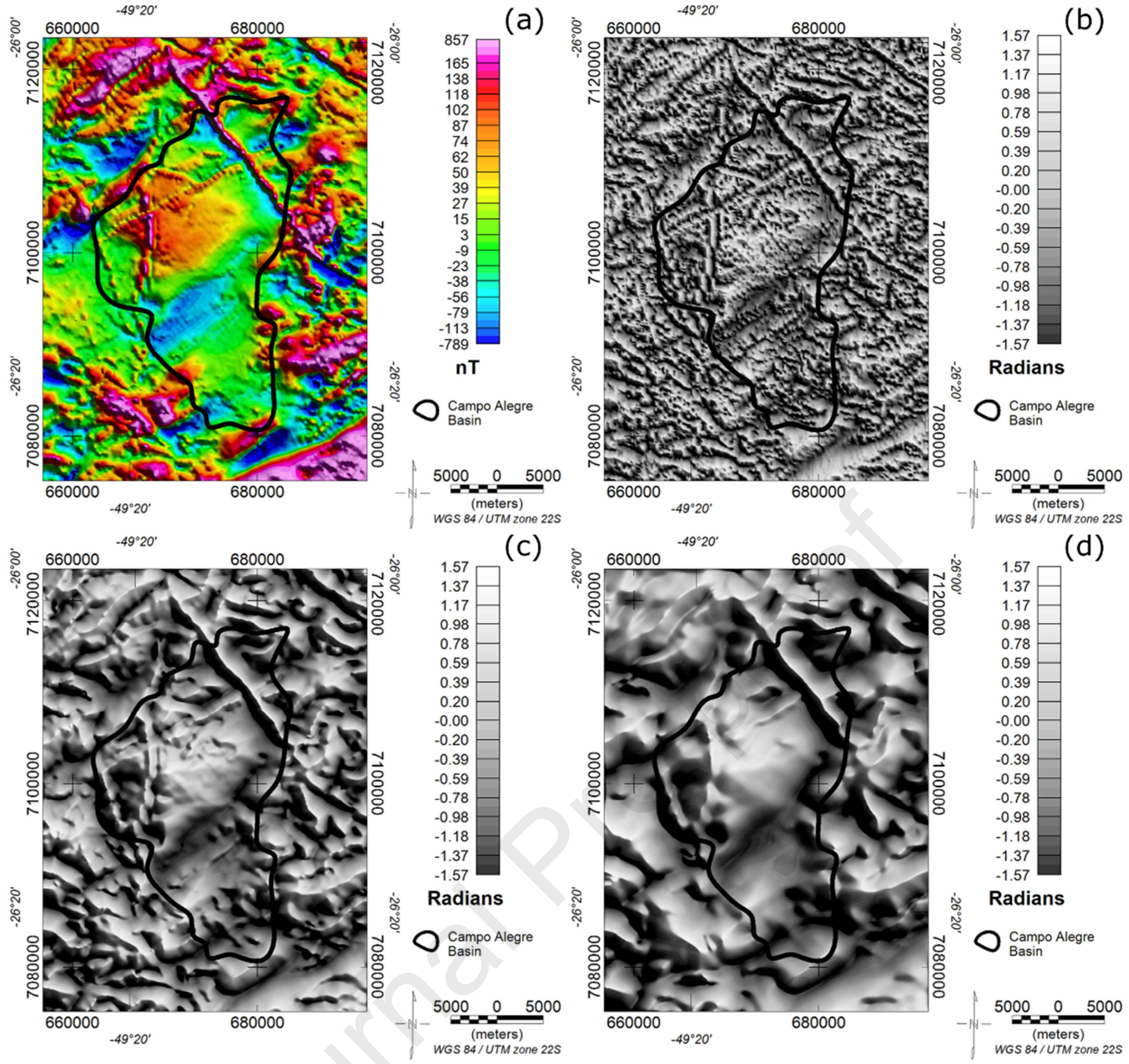

Figure 6: *(a) Anomalous Magnetic field of the Campo Alegre Basin. (b) Tilt Derivative filtering and the same filter after upward continue the magnetic field at (c) 500 m and (d) 1000 m.*

Table 1*: Lineament classification according to the filters used*

Lineament	Geological equivalence	Filtering
Short wavelength	Near-surface structures; mostly brittle	Tilt Derivative
Medium wavelength	Structures formed in local tectonic events	500 m Upward Continuation + Tilt Derivative
Long-wavelength	Deeper crustal structures formed during regional tectonic events	1000 m Upward Continuation + Tilt Derivative

In the region of the CACB, the long-wavelength lineaments represent not only deeper structures but also those that extend from shallow to deep crustal horizons. These long-wavelength lineaments are mainly following the major N60°Az trend observed in the region (**Fig.7a**). However, other sets occur crosscutting orthogonally the major trend, summed up by the strong lineaments seen directly in the anomalous magnetic field, limiting the southwest border of the CACB, and crossing its western portion in the north-south direction. Based on Euler deconvolution, depth estimates of the observed lineaments indicate that most of them appear less than 100 m below the surface, except those present at the central region of the CACB (**Fig.7b**). These estimates support the hypothesis that the structures, which generate the long-wavelength magnetic lineaments, starts at or nearly the exposed surface and extend into deep crustal levels. On the other hand, the deeper structures correspond to the short-wavelength lineaments, occurring mainly at the central portion of the CACB (**Fig.7b**), sectioning this basin into two domains, a NE-SW-striking segment in the north and another NNW-SSE-striking segment in the south.

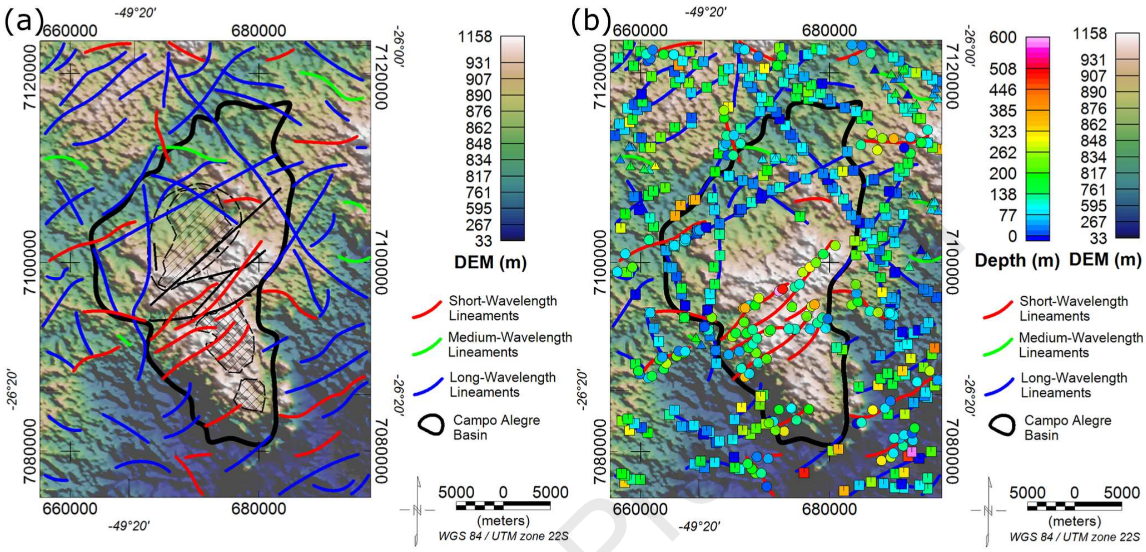

Figure 7: *(a) Digital elevation model of the Campo Alegre Basin area superposed by the classified magnetic lineaments. Dashed areas correspond to intra- and extra-caldera deposits. (b) Estimated depths of the shallower portions of the lineaments.*

5. Geomorphological and structural characterization

The CACB exhibits a peculiar geometry, nowadays occurring as an L-shaped basin with the major and the intermediate axis following the general NNW-SSW and NE-SW directions, respectively (**Fig.8**). Additionally, the Corupá sub-Basin and the Guaratubinha Basin both follow the same NE-SW orientation defined by the northern portion of the Campo Alegre Basin. Based on this geometrical partitioning of the CACB and the different basement units, we define three structural domains, namely the SW- and E-Zones, comprising the Paleoproterozoic SCGC, and the NW-Zone comprising the Neoproterozoic Piên Suites (**Fig.8a**). The SCGC defines the average elevation in the northern region of the CACB, around 800 to 850 meters high, and the lowest elevations to the southern areas, of about 100 to 200 meters (**Fig.8a**). On the other hand, the Neoproterozoic units occupy the highest elevations whatsoever in the study area, ranging from 950 to 1,200 meters, sustained by the granitoids from the Graciosa Province and the silicic volcanic rocks from the CACB, which occurs as a plateau in the region. Despite defining an almost flat highland, the volcanic sequences exhibit a subtle morphological pattern characterized by a more elevated ring of cuestas surrounding a northern depression in the northern portion of the CACB, whereas the southern portion defines a plateau. The ring of cuestas constitutes an almost circular alignment of mountain ranges that gently dips inwards towards the central north depression (**Fig.8b**).

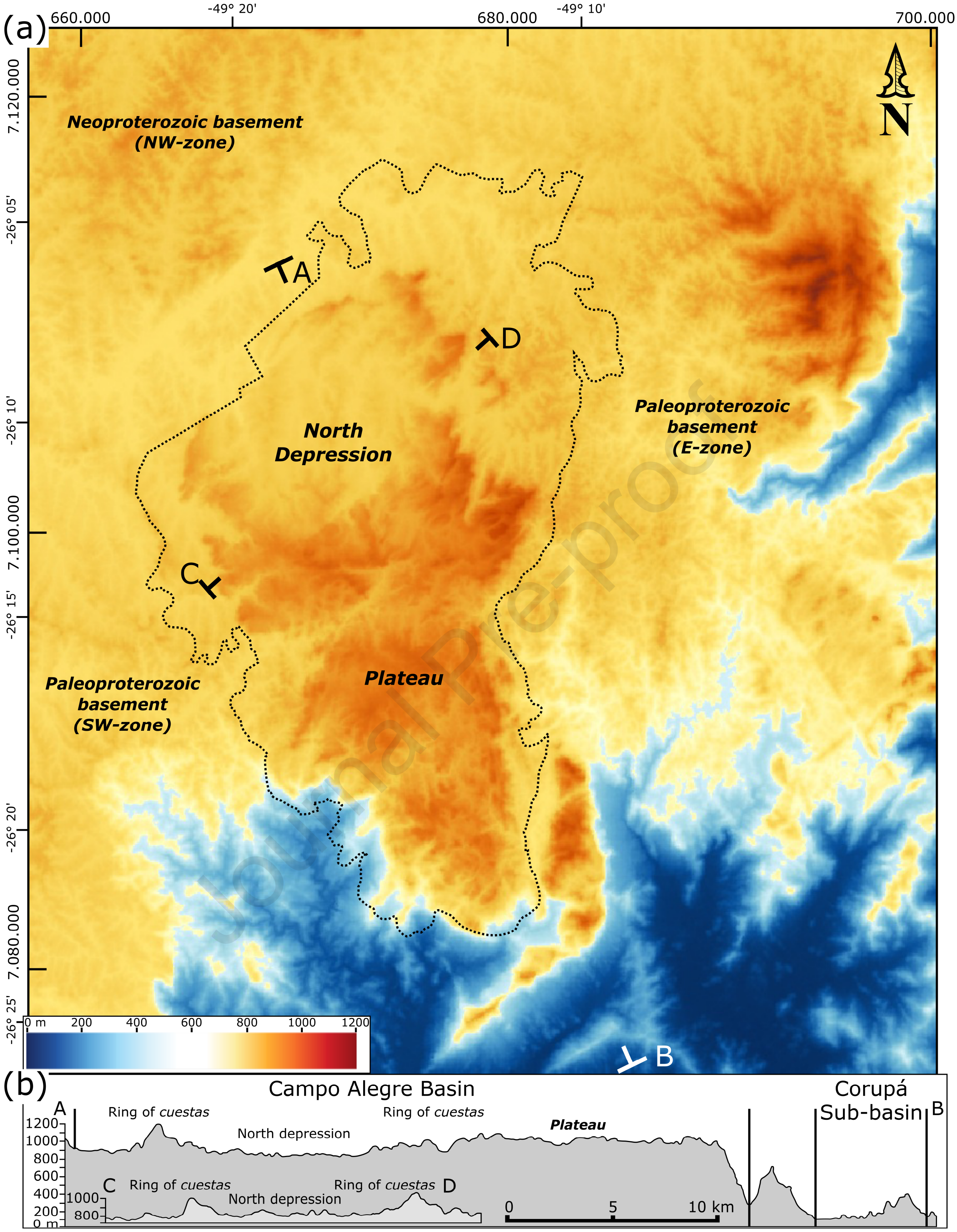

__Figure 8:__ (a) Digital elevation model of the Campo Alegre Basin region depicting the overall position of the basement zones and the internal distribution of topographic features including the North Depression, the Plateau, and the Ring of Cuestas. (b) Topographic profiles AB and CD exhibiting the geomorphological aspects of the North Depression and highlighting the Ring of Cuestas and the Plateau region in the Campo Alegre Basin. The Corupá Sub-basin occupies a depression in the south.

5.1. Structural framework of the CACB basement rocks

The structural framework of the LAT basement in the vicinities of the CACB, is characterized by significant variations in the orientation of gneissic foliations, resulting in two contrasting patterns of metamorphic anisotropies with almost orthogonal patterns. The first pattern is characteristic of the southwestern boundary of the CACB (**Fig.9a**), whereas the second pattern characterizes its eastern and northern limits in the basement E-Zone (**Fig.9b**). At the CACB western boundary, gneissic foliation shows an average direction of N15°W, dipping about 70°-80° to ENE. This sector also exhibits a subordinate gneissic foliation, with an average N26°W direction, dipping about 56° to SW (**Fig.9a**). Field structures such as asymmetric folds, with sub-horizontal fold-axis parallel to mineral lineation constituted by biotite and amphibole, suggest a local fold-and-thrust system with vergence to WSW (*cf.*, Harara, 2001). Additionally, the general orientation of gneissic foliation is progressively rotated in an anti-clockwise direction towards the north, resulting in N65°W oriented structures (**Fig.9a**).

At the CACB eastern boundary, the gneissic foliation is characterized by a general average direction of N80°E, dipping 65° to NNW, accompanied by a subordinate metamorphic foliation, exhibiting an average N82°E direction, dipping 65-70° to ESE. Asymmetric folds and other field structures suggest a local thrust and fold system, resulting in cylindrical ESE-WNW oriented folds with vergence to SSE. Towards the northern limit of the CACB, close to the Piên Shear Zone, the folded gneissic foliation rotates to N50°E, and the predominant dipping of about 65° changes the overall dip-direction to NW (**Fig.9b**). In the vicinities of the Piên Shear-Zone and near the Guaratubinha Basin, the gneissic foliation exhibits an average orientation of about N45-50°E, following the same pattern observed in the northern limit of the CACB. In both the SW- and E-Zones, these asymmetrical folded structures recognized in the medium- to high-grade metamorphic rocks from the LAT basement were possibly generated by deformation and metamorphism during granulite-facies events in the Paleoproterozoic (Basei *et al.*, 1998; Harara, 2001; Basei *et al.*, 2009). Later regional medium to low-grade retrometamorphic reactions induced by the Neoproterozoic orogenic cycle was possibly responsible for overprinting these structures within a predominant NE trend with vergence to SE (Basei, 1985; Harara, 1996; Harara, 2001).

The structural framework in the mafic-ultramafic and granitic Piên suites characterize the northern and northwestern border of the LAT, recording the collisional tectonics developed in the Neoproterozoic, and have a significant impact in the reactivation and generation of new structures in the SCGC. The Piên Mafic-Ultramafic Suite is interpreted as an obducted slice of oceanic lithosphere (*cf.*, Harara, 2001), characterized by an anastomosed to folded metamorphic schistosities, exhibiting an average foliation with N65°E dipping 22° to NW. Coupled to the main metamorphic structure, there is a down-dip mineral stretching lineation, exhibiting an average N25°W orientation and dipping 22° to NW, suggesting a vergence to SE (**Fig.9c**). On the other hand, the fabric developed in the pre- to syn-collisional granites from the Piên Magmatic Arc show a steeper foliation with an average orientation of N52°E, dipping 68° to NW (**Fig.9d**). The overall orientation of these Neoproterozoic suites is approximately parallel to the gneissic foliation of medium- to low-grade retrometamorphic rocks of the SCGC at the northern boundary of the CACB and in the vicinities of Guaratubinha Basin, following the orientation of the Piên Shear Zone.

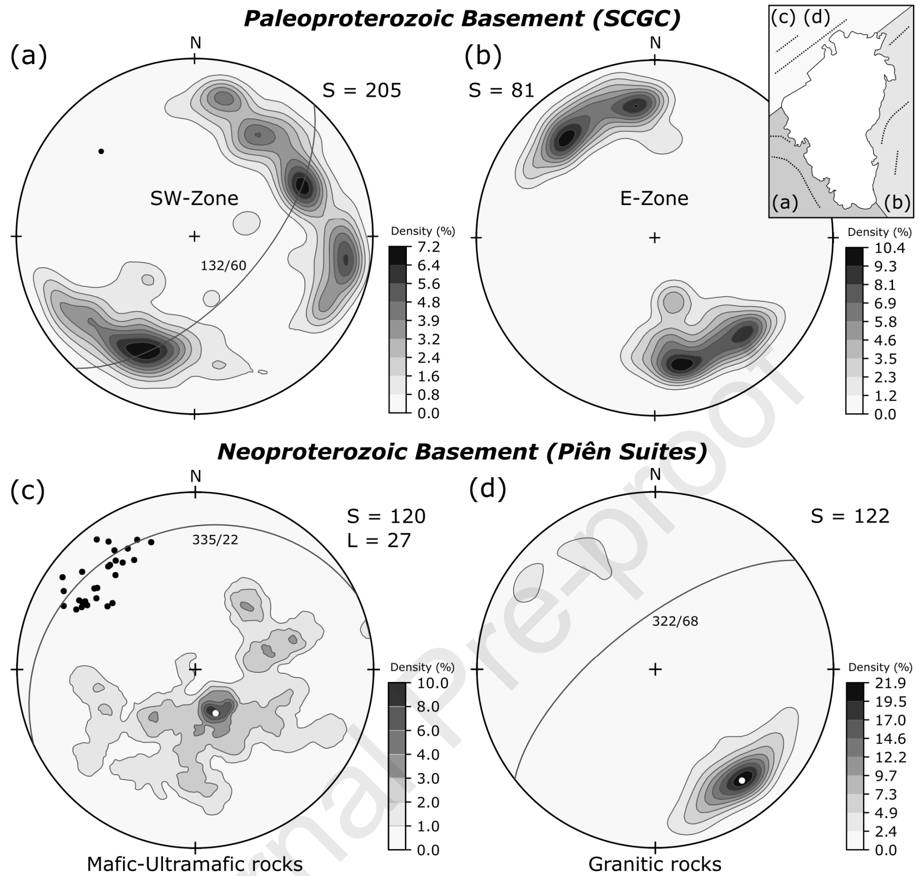

Figure 9: *Equal area lower-hemisphere stereograms for deformational structures. (a) Paleoproterozoic basement structures from the SCGC (SW-Zone) illustrating the main metamorphic structures. Data from Harara (2001) and this study. The fold axis estimation and fold-plane 132/60 (Dip-Direction/Dip) NE-SW-striking is based on field observations. (b) Paleoproterozoic basement structures from the SCGC (E-Zone) with E-W and NE-SW fold-planes. (c) Neoproterozoic basement structures from the Piên Mafic-Ultramafic Suite (NW-Zone). Note the average 335/22 NE-SW-striking foliation plane, containing most of the mineral stretching lineation, dipping to NW. (d) Neoproterozoic basement structures from the Piên Granitic Suite. Note the average NE-SW-striking 322/68 plane. The inset in (b) illustrates the geographical distribution of the structural zones in the basement.*

5.2. Depositional structures of the volcano-sedimentary sequences

Depositional structures from sedimentary and volcanogenic sequences in the CACB are in general sub-horizontal, with the exceptions of local moderate to steep structures (>35°), frequently related to high-angle faults from post-depositional events. The epiclastic sedimentary sequence as a whole exhibits massive structures, with rare clast imbrication, orientation, as well as grading or any type of stratification. Sedimentary bedding can be recognized in clast-supported conglomerates, marked by the grain size variation of pebbles and in the interbedded decimetric to metric layers of coarse-grained arcosean sandstones. In the upper braided-facies of arcosean sandstones, small-sized tabular cross-bedding, also including pelitic layers with horizontal plane bedding, marks the main sedimentary structures. It is possible to observe the predominance of low-angle bedding with gentle dips to SE and, a subordinately, to SW (**Fig.10a**). Additionally, paleocurrent structures indicate a predominance of sedimentary transport from NW towards SE and a second direction suggesting the transport from NE to SW. Both main paleocurrent structures are sub-parallel to the main and intermediate axis of the CACB.

The volcanogenic sequences, composed mainly by lava flows and pyroclastic sequences with minor volcanogenic sediments (*cf.*, Quiroz-Valle *et al.*, 2020), constitute the most abundant rock-types at the CACB and exhibit a varied range of bedding structures originated by flow and/or fall deposition. The overall orientation of these depositional structures is more dispersed than that of the epiclastic units (**Fig.10c**), with a considerable number of field measurements recording moderately to steep dipping beddings (>35°). Regarding the regional structural distribution, the volcanic units of the CACB can be subdivided into two geographical sectors V1 and V2 (**Fig.10**-inset). In the former, most horizontal bedding structures are distributed within the north depression, whereas there is a progressively increase in the average dipping towards the boundaries of the basin in the region of the ring of cuestas. In these regions, the average bedding of each zone tendentially dips towards the center of the north depression (**Fig.10c**), as also pointed out by Citroni *et al.* (2001). On the other hand, the depositional structures in the southern plateau exhibit a dominantly SE-wards dipping (**Fig.10d**).

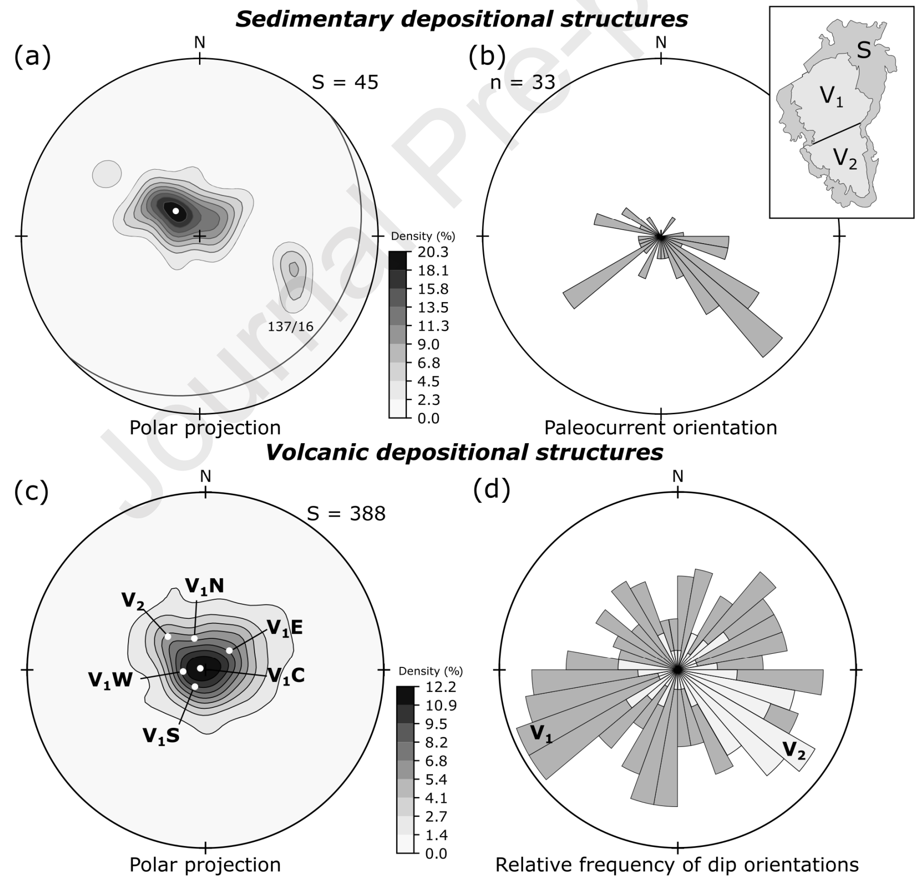

Figure 10: *Equal area lower-hemisphere stereograms and rose diagrams illustrating the orientation of depositional structures for (a-b) the sedimentary and (c-d) volcanic rocks in the CACB. The inset illustrates the geographical distribution of the sedimentary (S) and volcanic rocks from the northern (V_1) and southern (V_2) regions.*

5.3. Brittle structures in the volcano-sedimentary sequences

Most of the fault planes recognized in the volcanogenic and epiclastic sequences lack kinematic indication. However, based on the stratigraphic relationship of rock layers, it is possible to observe the predominance of normal faults over reverse faults. Strike-slip faults are almost absent within the basin, being largely present in the basement rocks from the Piên Suites and the SCGC. The faults within the CACB are generally characterized by planes with high- to moderate dip angles (between 35° and 85°), dipping mostly to NW, SE, and SW, exhibiting a preferred NE-SW-strike and dip orientation to SE (**Fig.11a**). There is also a significant NW-SE-striking group of faults (**Fig.11a**), dipping both to NE and to SW. These orientations are in contrast with that of dikes of both basic and acid compositions, commonly intrusive in basement rocks at the CACB boundaries. These dikes have strikes mostly oriented in the NNW-SSE and ENE-WSW directions, dipping on average to the east and south, respectively (**Fig.11b**). There is also a group exhibiting a NE-strike that is relatively less frequent but includes dikes tens of meters long.

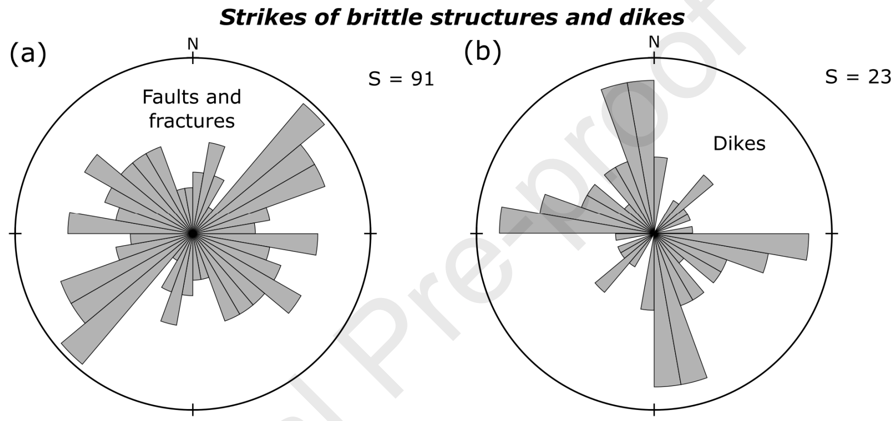

Figure 11: *Rose diagrams exhibiting the relative frequency of strikes orientation from (g) faults and fractures, and (h) dikes occurring in the CACB region.*

6. U-Pb geochronology

The obtained U-Pb zircon age results for both dated pyroclastic sequences are shown in **Figs.12a** and **12b**, representing samples taken from the bottom and sequences, respectively. Cathodoluminescence (CL) images of representative zircons from both samples are shown in Supplementary Material 2 (**Fig.S2)**, while individual LA-ICP-MC-MS spot analytical data are listed in Supplementary Material 3. In the analyzed samples, two distinguishable age clusters were recognized, the youngest at about 580-600 Ma and the oldest at about 2,200 Ma (**Fig.12**). The Neoproterozoic cluster is more expressive in the uppermost pyroclastic sequence, whereas the Paleoproterozoic group predominates in the lower pyroclastic occurrence. Zircon Th/U ratios are greater in the Neoproterozoic cluster, with mean values of about 1.88 (PPW-01) and 1.90 (PPW-03), ranging between 0.99 and 2.50. For the Paleoproterozoic cluster, Th/U ratios are usually < 1, ranging between 0.2 and 1.3 with mean values of about 0.64 (PPW-01) and 0.68 (PPW-03). Based on CL brightness, crystallographic and morphological aspects, the zircon crystals from the Neoproterozoic cluster were separated into three main zircon groups (ZG), of which ZG1 and ZG2 represent different generations of magmatic crystals restricted to sample PPW-01 and PPM-03, respectively, whereas zircons with hydrothermal features, recognized in both samples, were grouped into ZG3. For more details and additional information, see Supplementary Material 2.

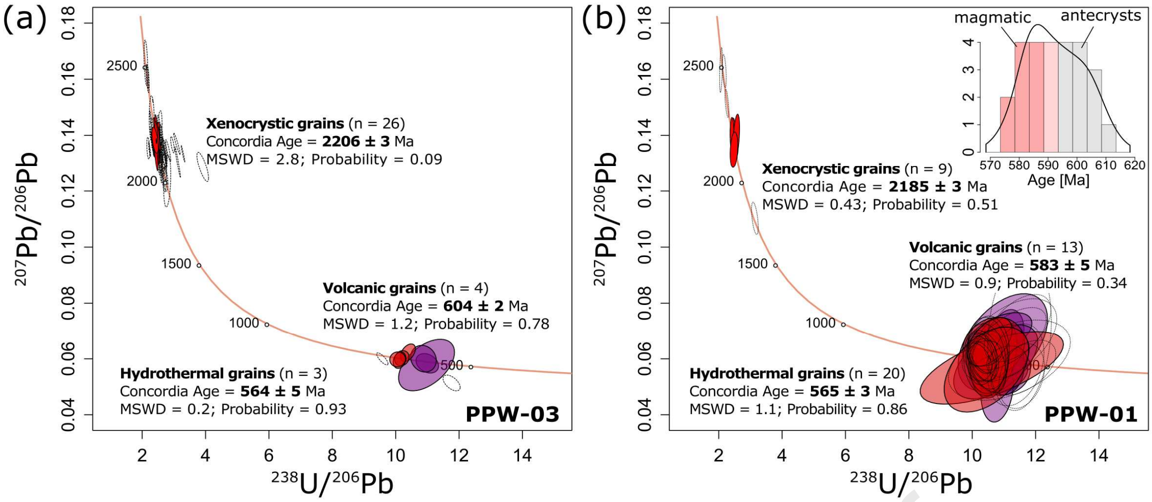

Figure 12: *LA-MC-ICP-MS U-Pb geochronological data depicting the obtained Concordia age for the lowermost pyroclastic event (a; n = 76) and the uppermost ignimbritic sample (b; n = 64). Inset in (b) represents the age distribution of crystals from the Main Volcanic Activity. Empty ellipses represent ages not considered in the calculation of the concordia ages. For more details, see the discussion section.*

U-Pb ages from the Neoproterozoic crystals are distributed in two clusters for both samples. In the lowermost unit (**Fig.12a**.), four crystals were characterized as corresponding to ZG2, yielding a concordia age of about 604 ± 2 Ma (MSWD = 1.2; prob. = 0.78). The remaining crystals correspond to ZG3, and result in concordia age of ~564 ± 5 Ma (n = 3; MSWD = 0.2; prob. = 0.86). On the other hand, the uppermost sequence yields a wide range of Neoproterozoic ages (**Fig.12b)**, in which 13 crystals characterized as ZG1 yield a concordia age of 583 ± 5 Ma (MSWD = 0.9; prob. = 0.34). This population has an almost two-peak distribution as depicted in a Kernel density plot (**Fig.12b** *inset*), suggesting different populations in which the oldest clusters around ca. 595 ± 3 Ma (n = 13; MSWD = 0.63; prob. = 1). On the other hand, the youngest crystals correspond to ZG3 and result in a concordia age at ~565 ± 3 Ma (n = 20; MSWD = 1.1; prob. = 0.86).

7. Discussions

7.1. Emplacement ages of the Initial and the Main Volcanic Activities

The selected samples for U-Pb dating are from widespread rock layers that mark significant changes in the depositional environment of the volcanic sequences and offer a general stratigraphic constraint for each depositional stage, that is, the *Initial* and *Main* volcanic activities. In a first approximation, similar concordia ages were obtained from the most abundant Paleoproterozoic age cluster in both samples, resulting in a range of ~2,206 - 2,185 Ma. Although neither of the analyzed samples exhibits accidental fragments from the basement rocks (*cf.*, Supplementary Material 2), there is evidence of accidental fragments from the surrounding metamorphic rocks and the conglomerates in the pyroclastic sequences (*e.g.*, Citroni *et al.*, 2001). Thus, we interpreted these zircon crystals as xenocrystic grains from the SCGC due to their similar U-Pb zircon ages (**Fig.12**). In this sense, the remaining results constrain the emplacement of the two dated pyroclastic layers in the Neoproterozoic, between ~605 Ma and ~565 Ma. Based on the geochronological data and textural aspects of the Neoproterozoic zircon crystals, it is possible to distinguish two main age intervals for these volcanic activities. The first one at

604 Ma was obtained in crystals from the ZG1 in sample PPW-03, whereas ZG2 in sample PPW-01 constraints a younger activity between ~595 Ma and ~583 Ma. An additional age group is common for both samples at 565 Ma, obtained in crystals from the ZG3. On the interpretation of this dataset, this might suggest an inherited nature for zircons from ZG1 and ZG2 from different sources, with a common emplacement age of both sequences at 565 Ma. However, the youngest age cluster does not coincide with any regional event, and the overlapping ages of both units imply in a relatively fast change in the depositional environment from sub-aqueous to sub-aerial.

In this sense, for the lowermost sample PPW-03, we interpret that the oldest concordia age cluster obtained in the Neoproterozoic group represents the emplacement age of the *Initial Volcanic Activity* at 604 ± 2 Ma. Conversely, for the uppermost sample PPW-01, we interpreted the youngest and most abundant normal-like age cluster (**Fig.12b**-inset) as the stage of crystallization of the *Main Volcanic Activity* occurring at 583 ± 5 Ma. This population can itself be divided into two clusters, the oldest of which (~595 ± 3 Ma) is herein interpreted as representing zircon antecrysts of this same event assimilated during the final pyroclastic activity, as constrained by the sampling of the topmost layers of the unit. This interpretation is supported by the presence of volcanic lithic fragments in this sample (*cf.* **Fig.S2e**). On the other hand, we interpret the age cluster obtained from zircon crystals of the ZG3 in both samples as a register of a widespread hydrothermal period, mostly due to their morphological aspects, in strong contrast with the remaining groups (ZG1 and ZG2). While the crystals of this population have characteristics that are not exclusive of hydrothermal crystals, the textural features observed in the smallest grains are identical to synthetic flux-grown crystals, frequently associated with hydrothermal origin (*e.g.*, Burakov *et al.*, 2002; McNaughton *et al.*, 2005; Schaltegger, 2007), especially crystallized from highly evolved alkaline granitic magmas (*cf.*, Yang *et al*., 2014). Additionally, both samples were collected within large rock expositions, close to normal faults and near to zones of Kaolin deposits at the upper volcanic sequences, and show further evidence of hydrothermal alteration (*cf.*, **FigS2**). The concordia ages presented above, considering uncertainties as 2σ, represent well-constrained ages, constituting intervals that do not overlap. They present reduced chi-squared deviations (MSWD) within an acceptable 2σ, considering each number of analyses, as expected for statistically robust interpretations (Spencer *et al.*, 2016). These intervals are coincident with other major local and regional events, further discussed in the next sections.

7.2. Quantification of 2D patterns of lineaments

A quantification of the two-dimensional structural patterns was conducted in the region of the CACB, combining both the obtained magnetic and geomorphological lineaments. The geographical distribution and the relative frequency of these structures are shown in **Fig.13** and insets. In general, the lineament patterns result in two principal sets at N5°Az and N55°Az, and a subordinated set at N135°Az. As observed, there is a predominance of the longest (> 30 km) lineaments as part of the N135°Az set, whereas the medium-sized (~20 km) lineaments constitute the N55°Az set and the shorter set of lineaments (< 15 km) constitute the N5°Az pattern. All sets of magnetic and geomorphological lineaments defined at the region of the CACB are following the local structuration of the LAT (**Fig.5**). However, most of the NE-SW lineaments seems to be restricted and more frequent in the CACB region. The sets of lineaments are parallel aligned to the main surrounding Neoproterozoic shear zones, which might suggest a contemporaneity between these structures.

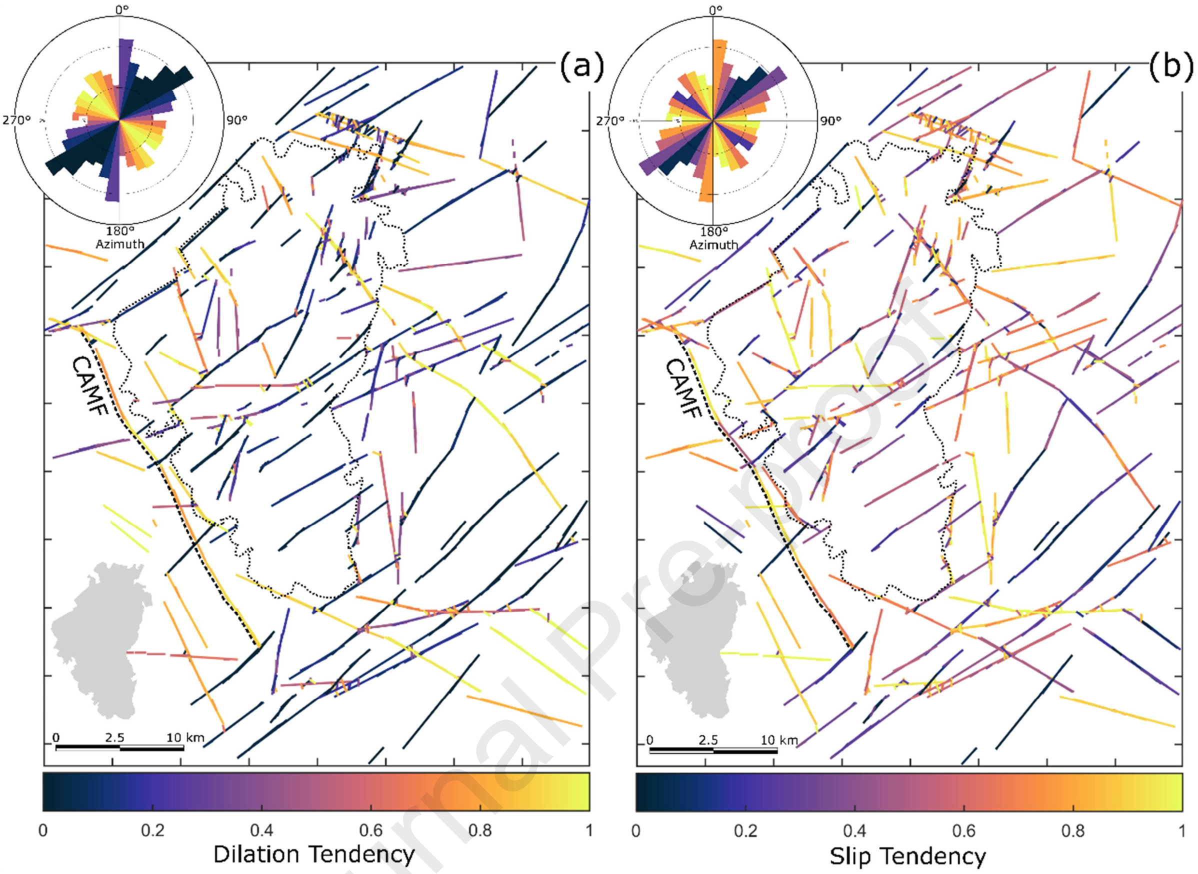

Figure 13*: Geographical distribution of geomorphological and geophysical patterns of lineaments and their relative frequency (inset rose-diagrams) in the region of the Campo Alegre-Corupá Basin, indicating the normalized (a) dilation and (b) slip tendencies for each lineament, considering a local σ1 at N150°Az. Grey polygon represents the geometry of the Campo Alegre Basin outlined by dashed lines. The dark dashed line corresponds to the Campo Alegre Master Fault (CAMF).*

Fig.13 also investigates the structural behavior of the lineaments sets recognized in the CACB assuming a regional tensional state of shortening (s1) at N150°Az, as suggested by the average orientation of mineral stretching lineation observed in the Piên suites (**Fig.9c**). As discussed below, this assumption is justified by the overlap between the ages of the Piên Magmatic Arc and the new constraints for the initial volcanic activity of the CACB presented in this work. We simulate differential stress considering σ_1 = 100 MPa and σ_2 = 50 MPa, revealing the overall tendency to dilation and slip for the main lineaments (**Figs.13a-b**). The dilation tendency is greater for the N130°Az set of lineaments, parallel with the main axis of the basin and coincident with the most significant normal faults at the CACB region, such as the CAMF. On the other hand, the slipping tendency exhibits a more erratic pattern, with the highest values at N5°Az, N70°Az, and N160°Az, coinciding with some strike-slip faults found at the Corupá Sub-Basin (*cf.*, **Fig.2**, Citroni *et al.*, 2001). In a first approximation, this general orientation of horizontal stresses can reproduce the same distribution of normal and slip faults, as observed in the region of the Campo Alegre Basin and Corupá Sub-Basin.

7.3. Structural framework and development of the Campo Alegre-Corupá Basin

Both the Campo Alegre-Corupá and Guaratubinha are fault-bounded basins in which their basement rocks exhibit a structural control clearly outlined by aerogeophysical data (Barão *et al.*, 2017; this study). These basins were deposited at different sectors of the LAT presumably during the same period, and they exhibit oblique orientations of their major axis, generally following the basement inherited-structures. In general, based on structural and geophysical data, the LAT basement can be partitioned into three main domains (**Fig.5**). The Sector I includes NE-SW-striking structures outlined by magnetic properties as lineaments, whereas in the central domain, the Sector II is characterized by NNW-SS and E-W to NE-SW-striking structures, also outlined by magnetic lineaments and identified in the field. Sector III, occurring at the southern region, represents the least affected area of the LAT basement during the Neoproterozoic, and reveals an oval-shaped geometry of structures and magnetic lineaments, defining the Pomerode orthogneisses, with structures reoriented to the NE-SW-striking pattern at the Itajaí Basin. In summary, the different lineaments and structural domains in the LAT reflect the interaction between an earlier Paleoproterozoic deformation, partially overprinted by Neoproterozoic structures, particularly along the boundaries of the terrane, close to NE-SW-oriented shear zones.

Our data are in accordance with previous structural observations in the region, such as the NE-SW oriented foliations in the Sector I (*e.g.,* Barão *et al*., 2017), and the NNW-SSE (*e.g.,* Basei *et al.*, 2009; Passareli *et al*., 2018), and NW-SE in the Sector II (**Fig.9**). The coincidence of the main lineaments bounding the CACB (**Figs.5** and **6**) with the structural configuration observed in the basement surrounding the basin (**Fig.9**) suggest that these structures were probably reactivated during the collisional tectonic setting in the Neoproterozoic, coupled with neo-formed E-W and NE-SW fault structures in the study area, controlling the opening of the CACB (*cf.*, **Fig.13**). The crustal depths of the main structures, estimated based on the wavelengths of the anomalous magnetic field (**Figs.5-7**), support the interpretation that they assisted the development of the CACB (**Fig.13**) and facilitated the rise of magmas to surface during the volcanic activities, as they are coincident with the strike orientation of dikes (**Fig.11b**). We interpret both inherited and neo-formed structures to have been active during the oblique collision of the LAT basement with the surrounding terranes, as the partitioning of deformation in sectors within the SCGC is coincident with the general orientation and strain partitioning of Neoproterozoic lineaments seem in the Paranaguá Terrane (*e.g.,* Cury, 2009; Patias *et al.*, 2019).

This partitioning of the collisional deformation was probably controlled by contrasting structural and compositional characteristics within the SCGC, as outlined by magnetic and gamma spectrometric data (**Fig.5**), resulting in a differential impact of reactivation and development of new structures in the LAT during the Neoproterozoic. In the case of sectors I and II, the contrasting rheological characteristics related to the occurrence of metamorphic rocks with presumably different compositions, together with the orientation of the main previous structures, influenced the development of the pull-apart depocenter in the Guaratubinha region (Barão *et al.*, 2017) and the NNW-SSE oriented rift in the Campo Alegre region (**Fig.13**). In the CACB, the initial sedimentation starts mainly at the northern limit of the CACB, controlled by the uplift associated with thrust front. This resulted in a fan system with poorly sorted conglomerates and breccias, containing clasts from the LAT basement and granitic fragments from the Piên Magmatic Arc (Citroni *et al.*, 2001; Quiroz-Valle *et al.*, 2019). The western boundary defined by the CAMF controlled the further process of subsidence and sedimentary infilling further to the south, during the installation and evolution of the rift system.

The structural framework outlined above is supported by the basal sedimentary infill that records the opening of the CACB. These units are characterized by immature sequences, occurring mostly at its exposed northern boundaries, progressively reworked inwards and southwards. Based on sedimentary maturity, the stratigraphic succession of sedimentary facies, and paleocurrent indications, Citroni *et al.* (2001) and Quiroz-Valle *et al.* (2019) interpreted the process of filling in this basin occurring from northwest to southeast, with some braided rivers running from west to east, which is in accordance with the sedimentary structures presented here (**Fig.10a-b**). Hence, our structural data coupled with previous information supports the hypothesis of a rift system at the CACB, in which the sedimentation started at the northern limit near the thrust front from NE to SW and the general transport of sediments occurs from northwest to south/southeast, following mostly the longer axis of the basin. During the evolution of the rift system, contributions of the western and eastern flanks in the development and subsidence of the CACB are progressively more significant with time. These structures further control the rise of magmas during the *Initial Volcanic Activity* (*cf.*, Citroni *et al.*, 2001; Quiroz-Valle *et al.*, 2019).

7.4. The Volcanic Activities and the stages of development of the CACB

The volcanic records in the CACB can be divided into two main stages of occurrence, both of which exhibiting different characteristics. The first comprises basaltic to andesite-basaltic lava flows, associated with minor trachytic and rhyolitic occurrences, which become more progressive towards the top of the sequence, occurring mainly intercalated with fine-grained sedimentary rocks, still during subaqueous conditions. These volcanic sequences define the *Initial Volcanic Activity,* constituted by mildly alkaline basic to acid rocks that present chemical characteristic akin to intraplate tectonic settings (Citroni, 1998; Waichel *et al.*, 2000). The silicic occurrences are displayed mostly at the top of the basic to intermediate lava flows, occurring at the eastern and western boundaries of the CACB. Their emplacement was probably assisted by faults at the flanks of the basin during its initial rift stage, in which most of the deep-seated structures were reactivated (**Fig.5a**). The sedimentary and effusive volcanic rocks are both covered by the pyroclastic sequence of the Avenca Grande Formation, the last sequence of the *Initial Volcanic Activity*, constrained by our new data at ~604 ± 3 Ma (**Fig.12a**).

Recent results concerning the provenance characterization of the sedimentary sequences of the CACB suggest an early volcanic manifestation coeval with the development of the epiclastic deposits at ~606 ± 4 Ma (Quiroz-Valle *et al.*, 2019). A similar age constrains the emplacement of rhyolites from the Guaratubinha basin at ~605 ± 9 Ma (Basei *et al.*, 1998), which might represent an igneous manifestation contemporaneous with the basin development, as suggested by Barão *et al.* (2017). Considering the age intervals obtained in the pyroclastic rocks, and the local main Neoproterozoic tectonic events, the stage of the *Initial Volcanic Activity* at the CACB is well constrained as contemporaneous with the deposition of the basal epiclastic sequence. Our age constrains the period for the basin development and the *Initial Volcanic Activity* at ~606 - 604 ± 3 Ma, which coincides with the apex of the collisional stage in the region of the CACB, between ~615 - 595 Ma, as based on the crystallization ages of syncollisional granitoids and K-Ar regional cooling (Harara, 2001; Harara *et al.*, 2004).

The rift-stage sedimentary and volcanic manifestations are both covered by the much more voluminous acid magmatism of the CABC, the *Main Volcanic Activity*. This volcanism still preserves several occurrences and structures associated with the caldera-forming eruption and the syn-eruptive collapse process (*cf.*, Citroni *et al*., 2001). For instance, the general circular distribution of densely welded to rheomorphic ignimbrites, co-ignimbritic breccias, collapse breccias, and trachytic flows and rhyolitic domes, following the ring of *cuestas* at the northern portion (Citroni *et al*., 2001; Quiroz-Valle *et al*., 2020), suggest that this region underwent the collapsed of a km-scaled caldera floor. Based on the general structuration of the volcanic rocks and related faults (**Figs.10c-d, 11**), there is a clear predominance of sub-horizontal beddings, especially in the uppermost sequences, whereas the possibly syn-volcanic faults present no preferential orientation. These features indicate the collapse and subsequent infilling of an almost circular structure at the north area of the basin, whereas the volcanic depositional structures in the southern area dip out-wards. There is no evidence of the collapse collar in the caldera area. However, the presence of some massive radial-oriented collapse breccias, at the northern central region, and the presence of coarse-grained co-ignimbritic breccias beyond the ring-hills (*cf.*, Citroni *et al.*, 2001), might suggest that the caldera structure could be larger than the nowadays-preserved circular structure, with almost 20 km in diameter.

The new U-Pb data presented in this contribution offer an age of ~583 ± 5 Ma for the uppermost pyroclastic sequence of the *Main Volcanic Activity*. This new age is added to available U-Pb zircon ages from rhyolites of the same unit, constraining the main volcanic activity in the CACB at ~598 ± 29 Ma and ~595 ± 16 Ma (Basei et al., 1998; Cordani et al., 1999), thus establishing an interval at ~595-582 Ma for the emplacement of the silicic volcanic manifestation within the basin. This interval is in accordance with a second population identified in the new data record an age of ~595 ± 3 Ma, interpreted as obtained from zircon antecrysts, that is, not crystallized from the ‘magma’ in which they are hosted, but which were grown earlier within the same magmatic system. These crystals might represent the interval of initiation of silicic volcanism, compatible with age constraints previously reported for effusive sequences and some plutonic occurrences (*e.g.,* Basei et al., 1998; Cordani et al., 1999, Harara, 2001). In fact, the interval established for the *Main Volcanic Activity* is contemporaneous with the intrusion of the nearby granites from the Graciosa Province. Based on U-Pb zircon ages from granites and rhyolites from the Guaratubinha and the CACB, Basei *et al.* (2009) have constrained the magmatic activity in the Serra do Mar Suite (*i.e.*, Graciosa Province) at ~588 ± 5 Ma. More recently, Vlach *et al.* (2011) and Vilalva *et al*.

(2019) presented a reviewed interpretation for the crystallization stage of granites and syenites from the Graciosa Province, suggesting a short interval within a maximum period of ~ 9 Ma, peaking at 580-583 ± 3 Ma. This contemporaneity between the intrusive and volcanic magmatism, together with their similar chemical compositions (Lino *et al.*, 2020), might suggest the co-genetic nature of these volcanic and plutonic sequences.

The overall distribution of the volcanic rocks along the rift-controlled NNW-SSE long axis of the basin, together with the geometry and orientation of the ring-hills at the northern NE-SW segment, suggest that the regional tectonics and pre-existing rift-related structures influenced in the collapse of the caldera, as seen in other occurrences (Acocella *et al*., 2004; Acocella, 2007; Robertson *et al.*, 2016). Furthermore, the NNW-SSE and ENE-WSW structures in the Campo Alegre region controlled the intrusion of the feeder dikes (**Fig.11b**) and might have controlled the emplacement of the southernmost granites and syenites of the Graciosa Province as well (**Fig.1**). Northeastwards, inherited NE-SW basement structures might have also controlled the collapse of a section of the nested caldera or part of the caldera complex in the Guaratubinha region, presumably. These NE-SW inherited anisotropies probably control the intrusion of the NE-SW oriented occurrences from the Graciosa Province (Kaul and Cordani, 2000). Besides, the collapse breccias along with collapse faults may have assisted the hydrothermal circulation within the caldera ring, for which our new U-Pb data suggest a peak of activity at ~565 ± 5 Ma. Within the CACB, evidence for hydrothermal activity is widespread, as evidenced by the Kaolin deposits mostly in the rock sequences from the post-collapsed caldera (Biondi *et al.*, 2001a-b; Biondi *et al.*, 2002; Oliveira *et al.*, 2007). Hydrothermal overprint leading to partial Pb loss in the Neoproterozoic has also been recognized in basement rocks of the LAT close to the southwestern border of the CACB, strengthening the interaction between the basement and cover structures proposed here (Heller *et al.*, this volume).

8. Summary model and regional implication

Based on the novel results and interpretations, combined with previously reported regional data, we can summarize the origin and evolution of the volcano-sedimentary sequences in the region of Campo Alegre dividing them into the *Basin Stage* and the *Caldera Stage*. The nearly E-W rifting process gave rise to the *Basin Stage*, probably causing the associated strike-slip movements with NE-SW extension in the Guaratubinha Basin. Both probably result from the interaction between the inherited structural controls, marked by the orientation of basement anisotropies, with strain partitioning due to the irregular geometry of the LAT basement. Intraplate rifts and pull-apart basins, occurring as a response to Andean far-field stresses and more frequently as a response to continental collisional processes in general, are largely reported in the literature (*cf.*, Sengör, 1976; Burke *et al.*, 1985; Burke and Lytwyn, 1993; Visser and Praekelt, 1998; Liu *et al.*, 2013; Gianni *et al.*, 2015).

Intraplate rift/transtention induced by collisional processes (impactogenes in the sense of Sengör (1976)) may form in either proforeland (*e.g.* Rhine Graben) or retroforeland (*e.g.* Baikal Rift). Several factors can influence the origin and evolution of foreland basins, especially in the case of orogenic-triggered foreland rifting (Sengör, 1976; Sengör *et al.*, 1978; Liu *et al.*, 2013; Gianni *et al.*, 2015). However, collision-related rifts (*i.e.* Impactogenes) are distinguishable by a foreland rifting/transtension, presenting spatial and temporal relation to orogeny evolution and generally exhibiting orthogonal to oblique orientation with the orogenic system. Syn-extensional magmatism in the form of mafic dikes and alkaline volcanism are also distinctive features of these basins (Sengör, 1976; Visser and Praekelt, 1998; Liu *et al*., 2013; Gianni *et al*., 2015). The development of intra-plate rifts during collisional processes are controlled by (1) high-rates of convergence between plates within an oblique collision; (2) the thermal state and stress transmission by the foreland lithosphere, preferentially a cold lithosphere to inhibit strain absorption; (3) the collision between continents with irregular margins; (4) lithospheric domes in the hinterland zones; and (5) inherited basement structures, mostly at high angles from the collisional front (Sengör, 1976; Schumacher, 2002; Gianni *et al.*, 2015; Renda *et al.*, 2019).

The *Basin Stage* in the CACB, as supported by the obtained geochronological and structural data, can be interpreted as an orogenic-induced foreland rift in the sense of Gianni *et al.* (2015), which might represent an *impactogene* in the sense of Sengör *et al.* (1978). Following the most accepted model for the collisional process between the Luis Alves and Curitiba Terranes, the Piên Magmatic Arc was developed at the margin of the Curitiba Terrene, starting at ~620 Ma and lasting until ~610 Ma (**Fig.14a**). Deformed syncollisional granitoids (**Fig.9d**) were emplaced between ~605 Ma and ~595 Ma, contemporaneous with the sedimentation of the Bateias Formation at ~606 Ma (Harara, 2001; Cury, 2009; Quiroz-Valle *et al*., 2019). As indicated by the structural configuration in the Piên Mafic-Ultramafic Suite and Piên Magmatic Arc (**Fig.9c-d**), field evidence suggests a local (N150°Az) S-SE oriented front, thrusting onto the LAT basement at the northern boundary of the Campo Alegre basin at ~615-595 Ma (Harara, 2001; Harara *et al.*, 2004; Passareli *et al.*, 2018). This process interacted with the basement anisotropies in the region of the CACB, which can be grouped in two main sets of gneissic foliation and schistosities, one preferentially NNW-SSE oriented at the basin western limit, and a second set NE-SW oriented at the eastern and north boundaries (**Fig.9a-b**). The irregular contour of the LAT, outlined by aerogeophysics, specifically at the northern limit, influenced a strain partitioning along the Piên Shear Zone, resulting in a thrust zone (collisional front) at its southern limit and a dextral transpressional shear-zone at the north (**Fig.14b**). The localized stress produced by the indentation of the magmatic arc during the collisional process resulted in a set of secondary tension perpendicular or at high angles from the compressional zone. The orientation of the compressional zone, coupled with inherited intraplate weaknesses, could lead to the development of this extensional basin as an orthogonal rift near to the orogenic front at its northern limit (*cf.*, **Fig.10a**).

Impactogens are usually characterized by large and highly subsiding rifts, associated with variable amounts of alkaline magmatic activity, sometimes represented by considerable volumes (*i.e.*, Rhine and Oslo rifts; Sengör, 1995). On the other hand, synorogenic foreland rifts are comparatively small and less subsiding, related to small or absent alkaline magmatism (*i.e.*, San Jorge Gulf and Lomas de Olmedo Basin; Gianni *et al.*, 2015). As reported for the Easter Rift of Kenya and the Rio Grande Rift, the synchronous volcanic activity exerts a major influence on rift sedimentation (Mack and Seager, 1990; Ebinger and Scholz, 2012). In the Campo Alegre Basin, the volcanic activity seems to have a minor influence during the main sedimentation process, being progressively more significant at the upper sequences and in the final stages of sedimentation (Citroni *et al*., 2001; Quiroz-Valle *et al*., 2019). In this scenario, the volcanic activity probably resulted from an asthenospheric upwelling during the process of lithospheric thinning mostly at the collisional apex, whereas the sedimentation might have initiated earlier. This model suggests a transition from the synorogenic foreland-rift to the *impactogene* (*s.s.*) setting, probably resulting from an increase in the rates of convergence between the Luis Alves and Curitiba Terranes. The minor and late occurrence of bimodal, mildly alkaline to transitional volcanic rocks during the basin stage is compatible with the interpreted tectonic configuration, which is characteristic of passive rifts (*cf.*, Merle, 2011).

The second period of development of the CACB is the *Caldera Stage*. It characterizes the post-collisional setting in this region, in the sense of Liégeois (1998), which is represented by both the A-type granites and syenites from the Graciosa Province, and the volcanic rocks from the CACB and other occurrences at the Guaratubinha Basin and the northern limit of the Morro Redondo Massive (**Fig.14c**). A-type magmatism is a typical feature of anorogenic settings but has been frequently associated with extensional post-collisional tectonic scenarios as well (Bonin, 2007). The genesis of these A-type magmas might include lithospheric delamination, asthenospheric upwelling, and in some instances the metasomatic enrichment of the sub-continental lithospheric mantle of the upper plate. Recent petrogenetic models involving the partial melting of either metasomatized lower crust or lithospheric mantle are more frequent in the current literature (Aldanmaz *et al*., 2000; Martin, 2006; Sheng *et al*., 2011; Li *et al*., 2014; Jiang *et al*., 2018; Lin *et al*., 2020). In the case of the post-collisional magmatism of the *Caldera Stage* and the Graciosa Province, several authors discuss the probable influence of a mantle enrichment due to previous subduction process in the origin of these volcanic and plutonic rocks (*e.g.*, Waichel *et al*., 2000; Sommer *et al*., 2006; Vilalva *et al*., 2019). Here we interpret an episodic process of lithospheric extension, localized in a first moment during the basin development, induced by the collisional tectonics, and more generalized later during the post-collisional stage. Both extensional events might induce lithospheric thinning and asthenospheric upwelling causing "*intraplate-like*" magmatism. However, further and more detailed characterization of these volcanic occurrences and their association with intrusive granitoids occurring around the CACB is still needed.

Calderas are variable in shape and size, occurring mainly as semi-circular structures or forming caldera complexes, and they usually include some typical elements as a collapse collar, associated ring faults, and landslide breccia, and the intra-caldera ignimbritic sequences (Nairn *et al.*, 1994; Lipman, 2000; Cole *et al.*, 2005; Branney and Acocella, 2015). In the case of peralkaline and rhyolitic caldera-types, they are typically associated with zones under extensive tectonic settings, frequently constituting multiple calderas or caldera complexes. These caldera-types are usually associated with large amounts (>30 km^3) of pyroclastic and effusive sequences, preserved into depressions with >10 km in diameter that went through >1 km of subsidence of the caldera floor, reaching up to >4 km due to continued collapse (Acocella *et al.,* 2002; Bachmann *et al.*, 2002; Cole *et al*., 2005).

In the CACB, the preserved geomorphological feature resembling a volcano-caldera occurs at the northern portion of the rift system, occurring as a semi-circular structure, comprehending a mountain range and the north depression. This ring of cuestas presents almost 20 km in diameter, constituted by a thick (> 200 m) pile of pyroclastic and effusive volcanogenic rocks (**Fig.3c-f**). The extent of subsidence in this caldera is poorly known but the volume of pyroclastic rocks and lava flows, accounting for > 30 km^3 based on their areal extent and average thickness, is suggestive of the occurrence of large caldera-forming eruptions as seen elsewhere (*e.g.,* Lipman, 2000; Acocella *et al.*, 2000; Cole *et al.*, 2005; Tomek *et al.*, 2016; Aragon *et al*., 2018). In this sense, taking into account the compositional characteristics of the main rock-types and the size of the caldera structure, the caldera-forming eruption and collapse in the CACB might have acted as a significant mechanism of subsidence in the region, preserving a large portion of the sedimentary and volcanogenic sequences. Caldera structures are commonly preserved as large depressed areas, which is the case of the northern sector of the CACB. However, the entire volcanic sequence constitutes the highlands in the region. In this sense, a differential weathering and erosion potential of the basement rocks in relation to the volcanic sequences may have led to a geomorphological inversion of the basement following post-orogenic or more recent uplift.

Caldera-forming eruptions and syn-eruptive collapse mechanisms are challenging to understand even for modern examples, but some anatomic characteristics can be recognized in some well-preserved ancient successions. A general cycle of caldera development includes at least four main stages (Lipman, 2000; Cole *et al.*, 2005). During the pre-caldera stage, the initial migration and accumulation of magma into shallow crustal levels is frequently preserved in the form of silicic lava flows/domes and small explosive eruptions. In the case of the CACB, this stage is probably initiated at ~595 Ma, with the occurrence of trachytic and rhyolitic lava flows and minor explosive pyroclastic sequences, as they characterize the lower deposits from the Serra de São Miguel Formation (Quiroz-Valle *et al*., 2020). On the other hand, the caldera subsidence is usually triggered by an extensive magma withdrawal starting in the central vent and migrating to ring vents (Beresford and Cole, 2000; Cole *et al.*, 2005). In the CACB, the caldera collapse probably occurs at ~583 Ma, as recorded in our U-Pb age in the upper pyroclastic sequences from the Serra de São Miguel Formation, coinciding with the interval of crystallization obtained in the surrounding granitoids (Vlach *et al.*, 2011; Vilalva *et al.*, 2019). Finally, the post-collapse stages include effusive volcanism and small explosive eruptions (Citroni *et al*., 2001), as well as an intensive hydrothermal activity late in the cycle (Biondi *et al.*, 2001a, b; Biondi *et al.*, 2002; Oliveira *et al.*, 2007). All of these cycles are registered in the form of contrasting sequences in the CACB, and the hydrothermal period coincident with the late caldera cycle is generalized, as it affects rocks from all previous events at late stages (~565 Ma).

Long after the volcanic evolution of the basin, the latest igneous activity preserved in the region of the CACB occurs during the opening of the South Atlantic Ocean and the emplacement of the Paraná

Magmatic Province, at about 134 Ma (*e.g.* Peate *et al.*, 1992; Thiede and Vasconcelos, 2010). The Ponta Grossa dike-swarm was able to intrude the rocks from the LAT, as well as the Ediacaran sedimentary and igneous sequences. In the region, part of the deep-seated structures developed during the Neoproterozoic was probably reactivated in the Mesozoic, also assisting the magma ascent during the development of the Paraná Large Igneous Province. These basic dikes exhibit oblique orientations to the main dike-swam northwards (**Fig.14d**), as outlined by the magnetic maps and supported by our field evidence.

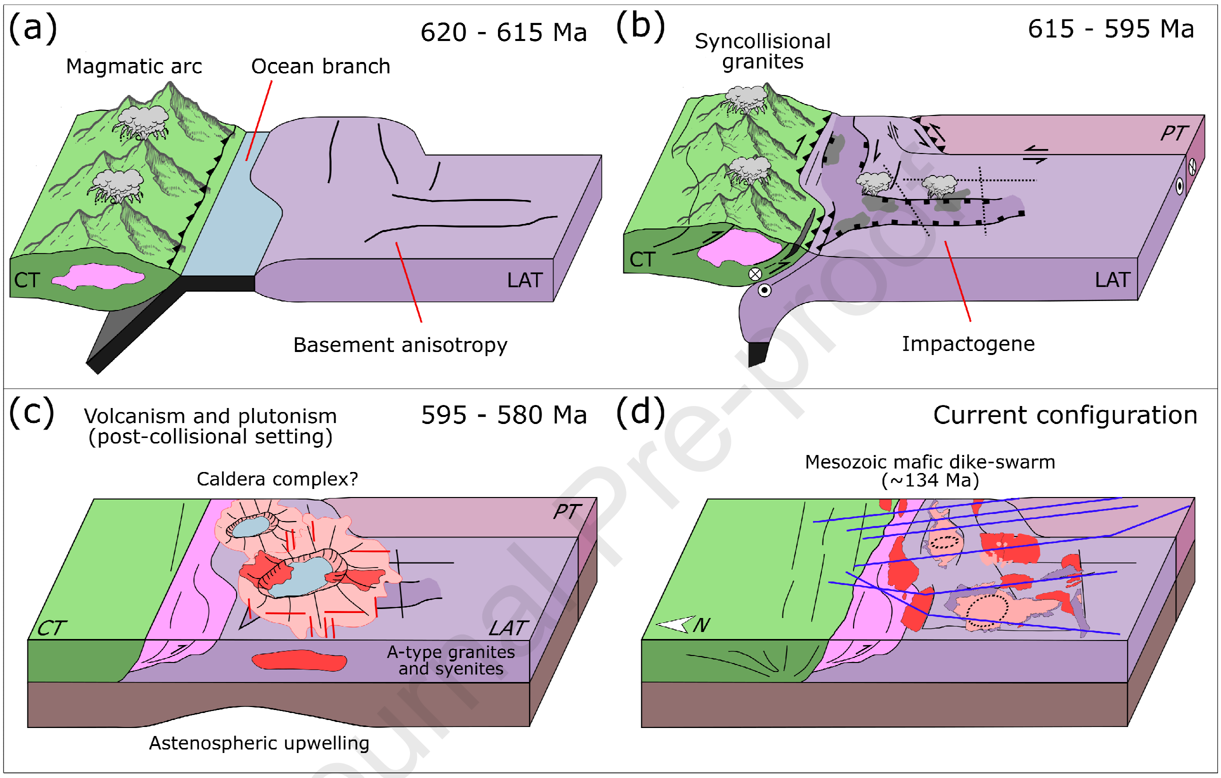

Figure 14: (a) Schematic model illustrating the collisional process between the Luis Alves Terrane (LAT) and the other near crustal blocks, the Curitiba Terrane (CT), and Paranaguá Terrane (PT), (b) giving rise to the Campo Alegre Basin. The post-collisional Caldera Stage (c) and latter Mesozoic dike-swarm (d) take place during contrasting extensional settings.

9. Concluding Remarks

The volcano-sedimentary sequences of Campo Alegre (i.*e.*, the *Sedimentary Basin* and the *Caldera Volcano*) comprehend snap-shots of different phases of the collisional and post-collisional tectonic setting in southern Brazil, as part of the late-orogenic stages of the Brasiliano event. Based on U-Pb geochronological results and the overall structural framework, as assessed by combined fieldwork and geophysical data, we conclude:

(1) The Campo Alegre volcano-sedimentary sequences represent the remnant of a collisional-triggered synorogenic foreland rift (*impactogene*), established at ~605 Ma, in the north boundary of the Luis Alves Terrane during the collisional tectonics. On the other hand, the post-collisional setting in the area probably initiated at ~ 595 Ma, as registered by the magmatic activity, followed by the installation of a caldera volcano with igneous activity peaking at ~ 583 Ma;

(2) The igneous manifestation in the caldera stage peak at ~583 Ma is comparable to the Graciosa Province, which might suggest a contemporaneous and co-magmatic occurrence. Additionally, the hydrothermal period registered in all rock sequences at ~565 Ma offer a young age limit for the volcanic activity in the caldera at this age, as the hydrothermal activity usually represent the latest event in the caldera cycle;

(3) Due to similarities in the sedimentary and volcanic sequences, as well as comparative ages, the Campo Alegre and Guaratubinha basins might have formed in response to the same compressional tectonic mechanisms during the Brasiliano orogeny. However, inherited basement structures and the irregular geometry of the LAT northern boundary, have certainly controlled their contrasting extensional development;

(4) The heterogeneities in the LAT basement were reactivated and new NNW-SSE and NE-SW deep-seated structures were developed during these late-orogenic processes in the Neoproterozoic, leading to the installation of a sedimentary basin. These deep-seated structures probably assisted the magma ascent during the *Initial Volcanic Activity*, and latter during the *Main Volcanic Activity*, as well as influencing the emplacement of some plutons from the A-type Graciosa Province;

(5) Previous works consider the Campo Alegre-Corupá and Guaratubinha Basins as part of a 1,500 km long Ediacaran to Cambrian rift system, starting at ~600 Ma (Almeida *et al.*, 2010, 2012). However, based on geochronological and structural data of the main regional events spatially related to the *Basin Stage* (Harara, 2001; Quiroz-Valle *et al.*, 2019; this study), we interpret its extensional evolution (*i.e.* NNW-rifting) with the compressive tectonic setting during the Brasiliano orogeny;

(6) The structures related to the basin development partially contributed to the latter mechanism of caldera collapse, and both events of subsidence (basin subsidence and caldera collapse) have a significant influence in the accumulated thickness of the volcano-sedimentary sequences, further influencing their preservation;

(7) Geochemical signatures of volcanic rocks are related to intra-plate to post-collisional settings, in the case of the basic and silicic volcanic rocks of the *Initial Volcanic Activity* (Waichel *et al.*, 2000). Moreover, the silicic effusive and explosive rocks from the *Main Volcanic Activity* are akin only to a post-collisional setting (Citroni, 1998; Waichel *et al*., 2000), which for instance might suggest a progressive transition in the tectonic settings (*i.e.,* continued extension) between these two magmatic manifestations;

(8) Finally, the contemporaneous occurrence of plutonic, sub-volcanic, and volcanic sequences during the post-collisional stage in the LTA open opportunities for the study of their genetic relationship and if these sequences might constitute a single volcanic and igneous plumbing system.

CRediT author statement

L.M. Lino: Conceptualization, Methodology, Investigation, Writing – original draft, Writing – review & editing, Formal analysis, Visualization. **F.R. Quiroz-Valle**: Conceptualization, Methodology, Investigation, Writing – original draft, Writing – review & editing, Formal analysis, Visualization. **V.H.A. Louro**: Methodology, Writing – original draft, Writing – review & editing, Formal analysis. **M.A.S. Basei**: Conceptualization, Methodology, Validation, Writing – review & editing, Resources, Supervision, Project administration, Funding acquisition. **S.R.F. Vlach**: Methodology, Supervision, Writing – review & editing. **M. Hueck**: Conceptualization, Methodology, Writing – review & editing. **P.R.M. Muñoz**: Methodology, Supervision, Writing – review & editing. **S.B. Citroni**: Methodology, Supervision, Writing – review & editing.

Declaration of competing interest

The authors declare that they have no known significant competing financial, professional, or personal interests that might have influenced the performance or presentation of the work described in this manuscript.

Appendix A. Supplementary Data

Acknowledgments

The authors thank the Fundação de Amparo à Pesquisa do Estado de São Paulo (FAPESP) for the financial support through the Thematic Project 2015/03737-0 (Coordinator Dr. M.A.S. Basei), and the Brazilian Geological Survey (CPRM) for permission to use aerogeophysical data. We are grateful to the CPGeo staff for support during the analytical procedures. LML thanks the *Conselho Nacional de Desenvolvimento Técnico e Científico* (CNPq – Grant 141624/2019-1) for the doctoral scholarship, FRQV thanks the *Coordenação de Aperfeiçoamento de Pessoal de Nível Superior* (CAPES – Grant 88882.377663/2019-01) for the master scholarship, and MH thanks the *Fundação de Amparo à Pesquisa do Estado de São Paulo* (FAPESP – Grant 2019/06838-2) for the postdoctoral scholarship. LML and FRQV thanks the Mocó Research Group for productive discussions, and Dr. Andrea Kern, and Dr. Bruno Becker Kerber for the review of the first version of the manuscript. We are grateful to Dr. Sebastián Oriolo and Dr. Pedro Oyhantçabal for editorial handling, and two anonymous reviewers for the criticism and the constructive comments about an earlier draft of this paper.

References

Acocella, V. (2007). Understanding caldera structure and development: An overview of analogue models compared to natural calderas. Earth-Science Reviews, 85(3-4), 125-160.

Acocella, V., Cifelli, F., & Funiciello, R. (2000). Analogue models of collapse calderas and resurgent domes. Journal of Volcanology and Geothermal Research, 104(1-4), 81-96.

Acocella, V., Funiciello, R., Marotta, E., Orsi, G., & De Vita, S. (2004). The role of extensional structures on experimental calderas and resurgence. Journal of Volcanology and Geothermal Research, 129(1-3), 199-217.

Acocella, V., Korme, T., Salvini, F., & Funiciello, R. (2002). Elliptic calderas in the Ethiopian Rift: control of pre-existing structures. Journal of Volcanology and Geothermal Research, 119(1-4), 189-203.

Aldanmaz, E. R. C. A. N., Pearce, J. A., Thirlwall, M. F., & Mitchell, J. G. (2000). Petrogenetic evolution of late Cenozoic, post-collision volcanism in western Anatolia, Turkey. Journal of volcanology and geothermal research, 102(1-2), 67-95.

Almeida, F. F. M., Hasui, Y., de Brito Neves, B. B., & Fuck, R. A. (1981). Brazilian structural provinces: an introduction. Earth-Science Reviews, 17(1-2), 1-29.

Almeida, R. P., Janikian, L., Fragoso-Cesar, A. R. S., & Fambrini, G. L. (2010). The Ediacaran to Cambrian rift system of Southeastern South America: tectonic implications. The Journal of Geology, 118(2), 145-161.

Almeida, R. P., Santos, M. G., Fragoso-Cesar, A. R., Janikian, L., Fambrini, G. L. (2012). Recurring extensional and strike-slip tectonics after the Neoproterozoic collisional events in the southern Mantiqueira province. Anais da Academia Brasileira de Ciências, 84(2), 347-376.

Aragon, E., Castro, A., Diaz-Alvarado, J., Pinotti, L., Fernando, D., Demartis, M., ... & Rodriguez, C. (2018). Mantle derived crystal-poor rhyolitic ignimbrites: Eruptive mechanism from geochemical and geochronological data of the Piedra Parada caldera, Southern Argentina. Geoscience Frontiers, 9(5), 1529-1553.

Bachmann, O., Dungan, M. A., & Lipman, P. W. (2002). The Fish Canyon magma body, San Juan volcanic field, Colorado: rejuvenation and eruption of an upper-crustal batholith. Journal of Petrology, 43(8), 1469-1503.

Barão, L. M., Trzaskos, B., Vesely, F. F., de Castro, L. G., Ferreira, F. J., Vasconcellos, E. M., & Barbosa, T. C. (2017). The role of post-collisional strike-slip tectonics in the geological evolution of the late Neoproterozoic volcano-sedimentary Guaratubinha Basin, southern Brazil. Journal of South American Earth Sciences, 80, 29-46.

Basei, M. A. S. (1985). O Cinturão Dom Feliciano em Santa Catarina (Doctoral dissertation, Universidade de São Paulo).

Basei, M. A. S., Frimmel, H. E., Neto, M. D. C. C., de Araujo, C. E. G., de Castro, N. A., & Passarelli, C. R. (2018). The tectonic history of the southern Adamastor Ocean based on a correlation of the Kaoko and Dom Feliciano belts. In Geology of Southwest Gondwana (pp. 63-85). Springer, Cham.

Basei, M. A. S., Frimmel, H. E., Nutman, A. P., & Preciozzi, F. (2008). West Gondwana amalgamation based on detrital zircon ages from Neoproterozoic Ribeira and Dom Feliciano belts of South America and comparison with coeval sequences from SW Africa. Geological Society, London, Special Publications, 294(1), 239-256.

Basei, M. A. S., McReath, I., & Siga Jr, O. (1998). The Santa Catarina granulite complex of southern Brazil: a review. Gondwana Research, 1(3-4), 383-391.

Basei, M. A. S., Neto, M. C., Castro, N. A., Nutman, A. P., Wemmer, K., Yamamoto, M. T., ... & Passarelli, C. R. (2011). Tectonic evolution of the Brusque Group, Dom Feliciano belt, Santa Catarina, Southern Brazil. Journal of South American Earth Sciences, 32(4), 324-350.

Basei, M. A., Siga Jr, O., Machiavelli, A., & Mancini, F. (1992). Evolução tectônica dos terrenos entre os Cinturões Ribeira e Dom Feliciano (PR-SC). Revista Brasileira de Geociências, 22(2), 216-221.

Basei, M.A.S., Nutman, A., Siga, O., Passarelli, C.R., Drukas, C.O., (2009). The Evolution and Tectonic Setting of the Luis Alves Microplate of Southeastern Brazil: An Exotic Terrane during the Assembly of Western Gondwana. Developments in Precambrian Geology, 273–291.

Basei, M.A.S., Siga Jr., O., Masquelin, H., Harara, O.M., Reis Neto, J.M., Preciozzi, F., (2000). The Dom Feliciano Belt of Brazil and Uruguay and its Foreland Domain the Rio de la Plata Craton: framework, tectonic evolution and correlation with similar provinces of Southwestern Africa. In: Cordani, U.G., Milani, E.J., Thomaz Filho, A., Campos, D.A. (Eds.), Tectonic Evolution of South America, pp. 311e334 (Rio de Janeiro).

Beresford, S. W., & Cole, J. W. (2000). Kaingaroa Ignimbrite, Taupo volcanic zone, New Zealand: evidence for asymmetric caldera subsidence of the Reporoa caldera. New Zealand Journal of Geology and Geophysics, 43(3), 471-481.

Biondi, J. C., Bartoszeck, M. K., & Vanzela, G. A. (2001a). Controles geológicos e geomorfológicos dos depósitos de caulim da bacia de Campo Alegre (SC). Revista Brasileira de Geociências, 31(1), 13-20.

Biondi, J. C., Bartoszeck, M. K., & Vanzela, G. A. (2001b). Análise da favorabilidade para depósitos de caulim na bacia de Campo Alegre (SC). Revista Brasileira de Geociências, 31(1), 59-66.

Biondi, J. C., Vasconcellos, E. M. G., & Vanzela, G. A. (2002). Estudo comparativo entre os minérios da Mina Bateias e de outras minas da região de Campo Alegre (Santa Catarina). Revista Brasileira de Geociências, 32(2), 245-254.

Bonin, B. (2007). A-type granites and related rocks: evolution of a concept, problems and prospects. Lithos, 97(1-2), 1-29.

Branney, M., and Acocella, V. (2015). Calderas. In The encyclopedia of volcanoes (pp. 299-315). Academic Press.

Brito-Neves, B. B. (2002). Main stages of the development of the sedimentary basins of South America and their relationship with the tectonics of supercontinents. Gondwana Research, 5(1), 175-196.

Brito-Neves, B. B. D., Campos Neto, M. D. C., & Fuck, R. A. (1999). From Rodinia to Western Gondwana: an approach to the Brasiliano-Pan African Cycle and orogenic collage. Episodes-Newsmagazine of the International Union of Geological Sciences, 22(3), 155-166.

Brito-Neves, B. B., & Cordani, U. G. (1991). Tectonic evolution of South America during the late Proterozoic. Precambrian Research, 53(1-2), 23-40.

Brito-Neves, B. B., Fuck, R. A., & Pimentel, M. M. (2014). The Brasiliano collage in South America: a review. Brazilian Journal of Geology, 44(3), 493-518.

Burakov, B. E., Hanchar, J. M., Zamoryanskaya, M. V., Garbuzov, V. M., & Zirlin, V. A. (2002). Synthesis and investigation of Pu-doped single crystal zircon,(Zr, Pu) SiO4. Radiochimica acta, 90(2), 95-97.

Burke, K. C., & Lytwyn, J. (1993). Origin of the rift under the Amazon basin as a result of continental collision during Pan-African time. International Geology Review, 35(10), 881-897.

Burke, K., Kidd, W. S. F., & Kusky, T. (1985). Is the Ventersdorp rift system of Southern Africa related to a continental collision between the Kaapvaal and Zimbabwe cratons at 2.64 Ga ago?. Tectonophysics, 115(1-2), 1-24.

Citroni, S. B. (1998). Bacia de Campo Alegre-SC: aspectos petrológicos, estratigráficos e caracterização geotectônica (Doctoral dissertation, Universidade de São Paulo).

Citroni, S. B., Basei, M. A., Siga JR, O., & Reis Neto, J. M. (2001). Volcanism and stratigraphy of the Neoproterozoic Campo Alegre basin, SC, Brazil. Anais da Academia Brasileira de Ciências, 73(4), 581-597.

Cole, J. W., Milner, D. M., & Spinks, K. D. (2005). Calderas and caldera structures: a review. Earth-Science Reviews, 69(1-2), 1-26.

Cordani, U. G., Basei, M. A. S., Siga Júnior, O., & Nutman, A. (1999). Idades U-Pb (SHRIMP) de rochas vulcânicas das Bacias de Campo Alegre, Itajaí e Castro (SC e PR). Anais da Academia Brasileira de Ciências, 71(4), 835.

CPRM, 2011. Projeto Aerogeofísico Paraná-Santa Catarina (PR, SC, SP). Companhia de Pesquisa de Recursos Minerais (CPRM), Serviço Geológico do Brasil. Comunicado sobre Dispon. dados Digit. aerogeofísicos (Magnetometria Gamaespectrometria) 1e14.

Cury, L. F. (2009). Geologia do terreno Paranaguá (Doctoral dissertation, Universidade de São Paulo).

Daitx, E. C. (1979). Contribuição ao conhecimento geológico dos depósitos molássicos relacionados à Região de Dobramentos Sudeste: 1-Bacia de Campo Alegre, SC. In: *Regional Geological Symposium* (Vol. 2, pp. 131-146).

Daitx, E., & Carvalho, M. (1981). Projeto geoquímica na área de Guaratubinha-Piên. Porto Alegre, DNPM/CPRM, 1, 184.

Druitt, T. H., & Sparks, R. S. J. (1984). On the formation of calderas during ignimbrite eruptions. Nature, 310(5979), 679-681.

Ebert, H., (1971). O Grupo Guaratubinha no norte do Estado de Santa Catarina. Congresso Brasileiro de Geologia, 25, São Paulo, 1971. Anais, São Paulo, SBG, 2, 153-157.

Ebinger, C., & Scholz, C. A. (2011). Continental rift basins: the East African perspective. Tectonics of sedimentary basins: Recent advances, 183-208.

Gianni, G. M., Navarrete, C. G., & Folguera, A. (2015). Synorogenic foreland rifts and transtensional basins: A review of Andean imprints on the evolution of the San Jorge Gulf, Salta Group and Taubaté Basins. Journal of South American Earth Sciences, 64, 288-306.

Girardi, V. A., & Ulbrich, H. H. G. J. (1978). A Sapphirine-Orthopyroxene-Spinel Occurrence In The Pien Area, Paraná, Southern Brazil. *Revista Brasileira de Geociências*, 8(4), 284-293.

Gualda, G. A., & Vlach, S. R. (2007). The Serra da Graciosa A-type Granites and Syenites, southern Brazil. Part 1: Regional setting and geological characterization. Anais da Academia Brasileira de Ciências, 79(3), 405-430.

Harara, O. M. (1996). Análise estrutural, petrológica e geocronológica dos litotipos da região da Pien (PR) e adjacências (Master dissertation, Universidade de São Paulo).

Harara, O. M. M. (2001). Mapeamento e Investigação Petrológica e Geocronológica dos Litotipos da Região do Alto Rio Negro (PR-SC): um exemplo de sucessivas e distintas atividades magmáticas durante o Neoproterozóico III (Doctoral dissertation, Universidade de São Paulo).

Harara, O. M. M., Basei, M. A. S., Siga-Jr, O., Campos-Neto, M. C. (2004). Neoproterozoic supra subduction zone (SSZ) ophiolitic rocks from Piên (PR), southern Brazil. Quarenta anos de geocronologia no Brasil. Boletim de Resumos, 89.

Hartmann, L. A., Silva, L. D., & Orlandi Filho, V. (1979). O Complexo Granulítico de Santa Catarina; descrição e implicações genéticas. Acta Geológica Leopoldensia, 3(6), 93-112.

Healy, D., Rizzo, R. E., Cornwell, D. G., Farrell, N. J., Watkins, H., Timms, N. E., Gomez-Rivas, E., Smith, M. (2017). FracPaQ: A MATLAB™ toolbox for the quantification of fracture patterns. Journal of Structural Geology, 95, 1-16.

Heller, B.M., Hueck, M., Passarelli C.R., Basei, M.A.S., In review. Zircon U-Pb geochronology and Hf isotopy of the Luís Alves Terrane: Archean to Paleoproterozoic evolution and Brasiliano overprint. Submitted to the *Journal of South American Earth Science* on August 7th 2020.

Hueck, M., Oyhantçabal, P., Philipp, R. P., Basei, M. A. S., & Siegesmund, S. (2018). The dom feliciano belt in southern Brazil and Uruguay. In Geology of Southwest Gondwana (pp. 267-302). Springer, Cham.

Jiang, X. Y., Ling, M. X., Wu, K., Zhang, Z. K., Sun, W. D., Sui, Q. L., & Xia, X. P. (2018). Insights into the origin of coexisting A1-and A2-type granites: Implications from zircon Hf-O isotopes of the Huayuangong intrusion in the Lower Yangtze River Belt, eastern China. Lithos, 318, 230-243.

Kaul, P. F. T., & Cordani, U. G. (2000). Geochemistry of the Serra do Mar granitoid magmatism and tectonic implications, southern Brazil. Revista Brasileira de Geociências, 30(1), 115-119.

Li, D., He, D. F., Santosh, M., & Tang, J. Y. (2014). Petrogenesis of Late Paleozoic volcanics from the Zhaheba depression, East Junggar: insights into collisional event in an accretionary orogen of Central Asia. Lithos, 184, 167-193.

Liégeois, J. P. (1998). Preface - Some words on the post-collisional magmatism: Lithos, vv 45 pp. xv-xvii.

Lin, Y. C., Chung, S. L., Bingöl, A. F., Yang, L., Okrostsvaridze, A., Pang, K. N., Lin, T. H. (2020). Diachronous initiation of post-collisional magmatism in the Arabia-Eurasia collision zone. Lithos, 356, 105394.

Lino, L. M., Cavallaro, F. D. A., Vlach, S. R. D. F., & Coelho, D. C. (2018). 2D magnetometric modeling of a basic-intermediate intrusion geometry: geophysical and geological approaches applied to the Limeira intrusion, Paraná Magmatic Province (SP, Brazil). Brazilian Journal of Geology, 48(2), 305-315.

Lino, L. M., Quiroz-Valle, F. R., Vlach, S. R. F., & Basei, M. Â. S. (2020). El papel de la configuración geodinámica durante las etapas finales de amalgamación del Gondwana occidental en el estilo eruptivo, edad de ocurrencia y en la evolución química de las rocas volcánicas per-alcalinas de la Cuenca de Campo Alegre, Brasil - Parte 2. In: 1er Congreso Alvo, vol.1, Antofagasta, Chile, Abstracts, p 329.

Lipman, P. W. (2000). Calderas. Encyclopedia of Volcanoes, 643-662.

Liu, S., Su, S., & Zhang, G. (2013). Early Mesozoic basin development in North China: Indications of cratonic deformation. Journal of Asian Earth Sciences, 62, 221-236.

Louro, V. H. A., Mantovani, M. S. M., & Ribeiro, V. B. (2014). Magnetic field analysis of Morro do Leme nickel deposit. Geophysics, 79(6), K1-K9.

Louro, V. H., Cawood, P. A., Mantovani, M. S., & Ribeiro, V. B. (2017). Tectonic insights of the southwest Amazon Craton from geophysical, geochemical and mineralogical data of Figueira Branca mafic-ultramafic suite, Brazil. Tectonophysics, 708, 96-107.

Ludwig, K. R. (2001). SQUID 1.02: A user’s manual. Berkeley, Berkeley Geochronology Center, Spec. Publ. 2.

Ludwig, K. R. (2003). User's manual for isoplot 3.00, a geochronlogical toolkit for microsoft excel. Berkeley Geochronl. Cent. Spec. Publ., 4, 25-32.

Mack, G. H., & Seager, W. R. (1990). Tectonic control on facies distribution of the Camp Rice and Palomas Formations (Pliocene-Pleistocene) in the southern Rio Grande rift. Geological Society of America Bulletin, 102(1), 45-53.

Martin, R. F. (2006). A-type granites of crustal origin ultimately result from open-system fenitization-type reactions in an extensional environment. Lithos, 91(1-4), 125-136.

McNaughton, N. J., Mueller, A. G., & Groves, D. I. (2005). The age of the giant Golden Mile deposit, Kalgoorlie, Western Australia: ion-microprobe zircon and monazite U-Pb geochronology of a synmineralization lamprophyre dike. Economic Geology, 100(7), 1427-1440.

Merle, O. (2011). A simple continental rift classification. *Tectonophysics*, *513*(1-4), 88-95.

Miller, H.G., Singh, V., (1994). Potential field tilt – a new concept for location of potential field sources. Journal of Applied Geophysics, 32, 213-217.

Nairn, I. A., Wood, C. P., & Bailey, R. A. (1994). The Reporoa caldera, Taupo volcanic zone: source of the Kaingaroa ignimbrites. Bulletin of Volcanology, 56(6-7), 529-537.

Oliveira, M. T., Furtado, S., Formoso, M. L., Eggleton, R. A., & Dani, N. (2007). Coexistence of halloysite and kaolinite: a study on the genesis of kaolin clays of Campo Alegre Basin, Santa Catarina State, Brazil. Anais da Academia Brasileira de Ciências, 79(4), 665-681.

Paim, P. S. G., Chemale Jr, F., & Lopes, R. D. C. (2000). A bacia do Camaquã. Geologia do Rio Grande do Sul, 231-274.

Paim, P. S. G., Junior, F. C., & Wildner, W. (2014). Estágios evolutivos da Bacia do Camaquã (RS). Ciência e Natura, 36(3), 183-193.

Passarelli, C. R., Basei, M. A. S., Siga, O., & Harara, O. M. M. (2018). The Luis Alves and Curitiba terranes: continental fragments in the Adamastor Ocean. In Geology of Southwest Gondwana (pp. 189-215). Springer, Cham.

Patias, D., Cury, L. F., & Siga Jr, O. (2019). Transpressional deformation during Ediacaran accretion of the Paranaguá Terrane, southernmost Ribeira Belt, Western Gondwana. Journal of South American Earth Sciences, 96, 102374.

Peate, D. W., Hawkesworth, C. J., & Mantovani, M. S. (1992). Chemical stratigraphy of the Paraná lavas (South America): classification of magma types and their spatial distribution. Bulletin of Volcanology, 55(1-2), 119-139.

Pupin, J. P. (1980). Zircon and granite petrology. Contributions to Mineralogy and Petrology, 73(3), 207-220.

Quiroz-Valle, F. R., Basei, M. A. S., & Lino, L. M. (2019). Petrography and detrital zircon U-Pb geochronology of sedimentary rocks of the Campo Alegre Basin, Southern Brazil: implications for Gondwana assembly. Brazilian Journal of Geology, 49(1).

Quiroz-Valle, F.R., Lino, L. M., Basei, M. A. S. (2020). El papel de la configuración geodinámica durante las etapas finales de amalgamación del Gondwana occidental en el estilo eruptivo, edad de ocurrencia y en la evolución química de las rocas volcánicas per-alcalinas de la Cuenca de Campo Alegre, Brasil - Parte 1. In: 1er Congreso Alvo, vol.1, Antofagasta, Chile, Abstracts, p 332.

Reid, A. B., Allsop, J.M., Granser, H., Millett, A.J., Somerton, I.W., (1990). Magnetic interpretation in three dimensions using Euler deconvolution. Geophysics, 55, 80–91, doi: 10.1190/1.1442774.

Reid, A. B., Ebbing, J., Webb, S. J., (2014). Avoidable Euler errors—The use and abuse of Euler deconvolution applied to potential fields. Geophysical Prospecting, 62, 1162–1168, doi: 10.1111/1365-2478.12119

Reid, A. B., Thurston, J. B., (2014). The structural index in gravity and magnetic interpretation: Errors, uses, and abuses. Geophysics, 79(4), J61–J66, doi: 10.1190/GEO2013-0235.1

Renda, E. M., Alvarez, D., Prezzi, C., Oriolo, S., & Vizán, H. (2019). Inherited basement structures and their influence in foreland evolution: A case study in Central Patagonia, Argentina. Tectonophysics, 772, 228232.

Riccomini, C., Velázquez, V.F., Gomes, C.B., (2005). Tectonic controls of the Mesozoic and Cenozoic alkaline magmatism in the central-southeastern Brazilian Platform. In: Comin-Chiaramonti, P., Gomes, C.B. (Eds.), Mesozoic to Cenozoic Alkaline Magmatism in the Brazilian Platform. Edusp/Fapesp, São Paulo, 31-55.

Robertson, E. A. M., Biggs, J., Cashman, K. V., Floyd, M. A., & Vye-Brown, C. (2016). Influence of regional tectonics and pre-existing structures on the formation of elliptical calderas in the Kenyan Rift. Geological Society, London, Special Publications, 420(1), 43-67.

Schaltegger, U. (2007). Hydrothermal zircon. Elements, 3(1), 51-79.

Schumacher, M. E. (2002). Upper Rhine Graben: role of preexisting structures during rift evolution. Tectonics, 21(1), 6-1.

Sengör, A. C. (1976). Collision of irregular continental margins: Implications for foreland deformation of Alpine-type orogens. Geology, 4(12), 779-782.

Sengor, A. C., Burke, K., & Dewey, J. F. (1978). Rifts at high angles to orogenic belts; tests for their origin and the Upper Rhine Graben as an example. American Journal of Science, 278(1), 24-40.

Sengor, A. M. C. (1995). Sedimentation and tectonics of fossil rifts. Tectonics of sedimentary basins, 53-117.

Shen, X., Zhang, H., Wang, Q., Wyman, D. A., & Yang, Y. (2011). Late Devonian–Early Permian A-type granites in the southern Altay Range, Northwest China: petrogenesis and implications for tectonic setting of "A2-type" granites. Journal of Asian Earth Sciences, 42(5), 986-1007.

Silva Lara, H., Oyhantçabal, P., Wemmer, K., Hueck, M., Basei, M.A.S., Siegesmund, S., In review. The Sierra de Aguirre Formation: Post-Collisional Ediacaran Volcanism in the Southernmost Dom Feliciano Belt. Submitted to the *Journal of South American Earth Science* on July 4th 2020.

Silva, L. C., McNaughton, N. J., Armstrong, R., Hartmann, L. A., & Fletcher, I. R. (2005). The Neoproterozoic Mantiqueira Province and its African connections: a zircon-based U–Pb geochronologic subdivision for the Brasiliano/Pan-African systems of orogens. Precambrian Research, 136(3-4), 203-240.

Spencer, C. J., Kirkland, C. L., & Taylor, R. J. (2016). Strategies towards statistically robust interpretations of in situ U–Pb zircon geochronology. Geoscience Frontiers, 7(4), 581-589.

Teixeira, A. L., Gaucher, C., Paim, P. S. G., Fonseca, M. M., Parente, C. V., Silva Filho, W. F., & Almeida, A. R. (2004). Bacias do estágio da transição da Plataforma Sul-Americana. Geologia do Continente Sul-Americano: Evoluçao da obra de Fernando Flávio Marques de Almeida. Beca Produçoes Culturais, Sao Paulo, 487-537.

Thiede, D. S., & Vasconcelos, P. M. (2010). Paraná flood basalts: rapid extrusion hypothesis confirmed by new 40Ar/39Ar results. Geology, 38(8), 747-750.

Tomek, F., Žák, J., Holub, F. V., Chlupáčová, M., & Verner, K. (2016). Growth of intra-caldera lava domes controlled by various modes of caldera collapse, the Štiavnica volcano–plutonic complex, Western Carpathians. Journal of Volcanology and Geothermal Research, 311, 183-197.

Valiati, D. (1974). Projeto Sondagem Campo Alegre/74. Convênio CNEN/CPRM, 2, 66.

Vilalva, F. C. J., Simonetti, A., & Vlach, S. R. F. (2019). Insights on the origin of the Graciosa A-type granites and syenites (Southern Brazil) from zircon U-Pb geochronology, chemistry, and Hf and O isotope compositions. Lithos, 340, 20-33.

Vilalva, F. C., & Vlach, S. R. (2014). Geology, petrography and geochemistry of the A-type granites from the Morro Redondo Complex (PR-SC), southern Brazil, Graciosa Province. Anais da Academia Brasileira de Ciências, 86(1), 85-116.

Visser, J. N., & Praekelt, H. E. (1998). Late Palaeozoic crustal block rotations within the Gondwana sector of Pangea. Tectonophysics, 287(1-4), 201-212.

Vlach, S. R., Siga Jr, O., Harara, O. M., Gualda, G. A., Basei, M. A., & Vilalva, F. C. (2011). Crystallization ages of the A-type magmatism of the Graciosa Province (Southern Brazil): Constraints from zircon U-Pb (ID-TIMS) dating of coeval K-rich gabbro-dioritic rocks. Journal of South American Earth Sciences, 32(4), 407-415.

Waichel, B. L., de Lima, E. F., & Sommer, C. A. (2017). The alkaline post-collisional volcanism of the Campo Alegre Basin, southern Brazil: petrogenetic aspects. *Revista Brasileira de Geociências*, 30(3), 393-396.

Yang, W. B., Niu, H. C., Shan, Q., Sun, W. D., Zhang, H., Li, N. B., & Yu, X. Y. (2014). Geochemistry of magmatic and hydrothermal zircon from the highly evolved Baerzhe alkaline granite: implications for Zr–REE–Nb mineralization. Mineralium Deposita, 49(4), 451-470.

Highlights:

"Structural architecture and the episodic evolution of the Ediacaran Campo Alegre Basin (southern Brazil): Implications for the development of a synorogenic foreland rift and a post-collisional caldera volcano"

- The structural architecture of an orogenic induced rift has been documented in the collisional setting during the western Gondwana assembly.
- U-Pb zircon ages from volcanic sequences reveal two different igneous manifestations, one during the foreland synorogenic rifting and another during the post-collisional extensional tectonics.
- The post-collisional caldera-volcano and the A-type granites and syenites from the Graciosa Province are contemporaneous igneous manifestations.